

AD-A181 449

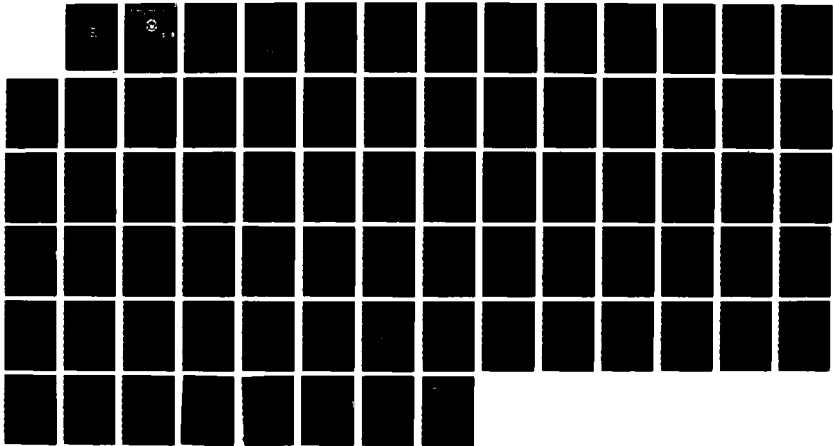
EXPERIMENTAL INVESTIGATION OF THE EFFECT OF CURVATURE
ON HEAT TRANSFER IN (U) NAVAL POSTGRADUATE SCHOOL
MONTEREY CA J R HAWK MAR 87

1/1

UNCLASSIFIED

F/G 28/13

NL



10
1.1
1.25
1.4
1.6
1.8
2.0
2.2
2.5

2

AD-A181 449

NAVAL POSTGRADUATE SCHOOL

Monterey, California

DTIC FILE COPY



DTIC
ELECTE
JUN 22 1987
S E D

THESIS

EXPERIMENTAL INVESTIGATION OF THE EFFECT
OF
CURVATURE ON HEAT TRANSFER IN A CURVED
RECTANGULAR CHANNEL OF HIGH ASPECT RATIO

by

John R. Hawk III

March 1987

Thesis Advisor

Matthew D. Kelleher

Approved for public release; distribution is unlimited.

AD B181-449

REPORT DOCUMENTATION PAGE

1a REPORT SECURITY CLASSIFICATION UNCLASSIFIED			1b RESTRICTIVE MARKINGS			
2a SECURITY CLASSIFICATION AUTHORITY			3 DISTRIBUTION/AVAILABILITY OF REPORT Approved for public release; distribution is unlimited			
2b DECLASSIFICATION/DOWNGRADING SCHEDULE			4 PERFORMING ORGANIZATION REPORT NUMBER(S)			
5a NAME OF PERFORMING ORGANIZATION Naval Postgraduate School			6a OFFICE SYMBOL (if applicable) 69		7a NAME OF MONITORING ORGANIZATION Naval Postgraduate School	
6c ADDRESS (City, State, and ZIP Code) Monterey, California 93943-5000			7b ADDRESS (City, State, and ZIP Code) Monterey, California 93943-5000			
8a NAME OF FUNDING, SPONSORING ORGANIZATION		8b OFFICE SYMBOL (if applicable)		9 PROCUREMENT INSTRUMENT IDENTIFICATION NUMBER		
8c ADDRESS (City, State and ZIP Code)		10 SOURCE OF FUNDING NUMBERS				
		PROGRAM ELEMENT NO	PROJECT NO	TASK NO	WORK UNIT ACCESSION NO	
11 TITLE (include Security Classification) EXPERIMENTAL INVESTIGATION OF THE EFFECT OF CURVATURE ON HEAT TRANSFER IN A CURVED RECTANGULAR CHANNEL OF HIGH ASPECT RATIO (UNCLASSIFIED)						
12 PERSONAL AUTHOR(S) Hawk, John R. III						
13a TYPE OF REPORT MS and Engineer Thesis		13b TIME COVERED FROM TO		14 DATE OF REPORT (Year Month Day) 1987 March		15 PAGE COUNT 75
16 SUPPLEMENTARY NOTATION						
17 COSAT CODES			18 SUBJECT TERMS (Continue on reverse if necessary and identify by block number)			
FIELD	GROUP	SUB GROUP	Taylor-Gortler Vortices, Duct Flow, Channel Flow, Curved Rectangular Channel, Secondary Flow, Heat Transfer, Dean Number,			
19 ABSTRACT (Continue on reverse if necessary and identify by block number)						
<p>An experimental investigation was conducted to study convective heat transfer in straight and curved rectangular channels of high aspect ratio that approximate plates of infinite extent. Experiments were performed at steady state in the turbulent flow regime with one wall held at a constant heat flux and the opposite wall essentially adiabatic. The effect of curvature induced secondary flow on heat transfer on the concave and convex walls was observed by comparing Nusselt numbers for four different configurations at several different Reynolds numbers. Significant heat transfer enhancement was observed on the concave wall. Correlations for Nusselt number as a function of Reynolds number were calculated for the cases studied.</p>						
20 DISTRIBUTION AVAILABILITY OF ABSTRACT <input checked="" type="checkbox"/> UNCLASSIFIED UNLIMITED <input type="checkbox"/> SAME AS RPT <input type="checkbox"/> DTIC USERS				21 ABSTRACT SECURITY CLASSIFICATION UNCLASSIFIED		
22a NAME OF RESPONSIBLE INDIVIDUAL Matthew D. Kelleher			22b TELEPHONE (include Area Code) (408)646-2530		22c OFFICE SYMBOL 69Kk	

Approved for public release; distribution is unlimited.

Experimental Investigation of the Effect of
Curvature on Heat Transfer in a Curved
Rectangular Channel of High Aspect Ratio

by

John R. Hawk III
Lieutenant, United States Navy
B.S.E.E., United States Naval Academy, 1978

Submitted in partial fulfillment of the
requirements for the degrees of

MASTER OF SCIENCE IN MECHANICAL ENGINEERING
and
MECHANICAL ENGINEER

from the

NAVAL POSTGRADUATE SCHOOL
March 1987

Author:

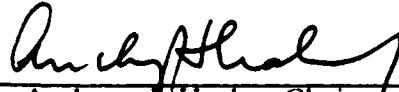


John R. Hawk III

Approved by:



Matthew D. Kelleher, Thesis Advisor



Anthony J. Healey, Chairman,
Department of Mechanical Engineering



Gordon E. Schacher,
Dean of Science and Engineering

ABSTRACT

An experimental investigation was conducted to study convective heat transfer in straight and curved rectangular channels of high aspect ratio that approximate plates of infinite extent. Experiments were performed at steady state in the turbulent flow regime with one wall held at a constant heat flux and the opposite wall essentially adiabatic. The effect of curvature induced secondary flow on heat transfer on the concave and convex walls was observed by comparing Nusselt numbers for four different configurations at several different Reynolds numbers. Significant heat transfer enhancement was observed on the concave wall. Correlations for Nusselt number as a function of Reynolds number were calculated for the cases studied.

Accession For	
NTIS GRA&I	<input checked="" type="checkbox"/>
DTIC TAB	<input type="checkbox"/>
Unannounced	<input type="checkbox"/>
Justification	
By _____	
Distribution/	
Availability Codes	
Dist	Avail and/or Special
A-1	



TABLE OF CONTENTS

I.	INTRODUCTION	12
	A. BACKGROUND	12
	B. APPLICATIONS	14
	C. INTENT OF THIS STUDY	14
II.	EXPERIMENTAL APPARATUS AND PROCEDURE	17
	A. DESCRIPTION OF THE APPARATUS	17
	B. EXPERIMENTAL PROCEDURE	20
III.	DATA REDUCTION	23
IV.	EXPERIMENTAL RESULTS	26
	A. HEATING THE STRAIGHT UPPER PLATE	26
	B. HEATING THE STRAIGHT LOWER PLATE	27
	C. HEATING THE OUTER CURVED (CONCAVE) PLATE	28
	D. HEATING THE INNER CURVED (CONVEX) PLATE	29
	E. EFFECT OF BUOYANCY	30
V.	DISCUSSION	42
	A. FLAT PLATES	42
	B. CURVED PLATES	43
VI.	CONCLUSION	46
VII.	RECOMMENDATIONS	47
	A. EQUIPMENT	47
	B. FURTHER RESEARCH	48
	APPENDIX A: DATA REDUCTION PROGRAM	49
	APPENDIX B: SAMPLE CALCULATION	60

APPENDIX C: EXPERIMENTAL UNCERTAINTY	68
LIST OF REFERENCES	72
INITIAL DISTRIBUTION LIST	74

LIST OF TABLES

1. SUMMARY OF STRAIGHT UPPER WALL RESULTS	31
2. SUMMARY OF STRAIGHT LOWER WALL RESULTS	32
3. SUMMARY OF CONCAVE WALL RESULTS	33
4. SUMMARY OF CONVEX WALL RESULTS	34

LIST OF FIGURES

1.1	Taylor Vortices Between Rotating Cylinders	13
1.2	Taylor-Gortler Vortices in a Curved Channel	15
2.1	Experimental Rectangular Channel	18
2.2	Thermocouple Placement in the Heated Plates	19
3.1	Power Measuring Circuit	24
4.1	Straight Upper Plate Results	35
4.2	Straight Lower Plate Results	36
4.3	Concave Plate Results	37
4.4	Comparison of Straight Upper and Concave Wall Results	38
4.5	Convex Plate Results	39
4.6	Comparison of Concave, Convex and Straight Plate Data	40
4.7	Convex/Concave Buoyancy Comparison	41

LIST OF SYMBOLS

<u>Symbol</u>	<u>Meaning</u>	<u>Units</u>
A	cross-sectional area of the orifice	m^2
A_c	cross-sectional area of the channel	m^2
A_{pipe}	cross-sectional area of pipe	m^2
A_{pl}	area of the heated plate	m^2
c_p	specific heat of air at constant pressure	$J/Kg \cdot ^\circ K$
D_c	channel height	m
De	Dean Number	
D_{hd}	channel hydraulic diameter	m
D_{orf}	flow measuring orifice diameter	m
D_{pipe}	diameter of the pipe	m
$F_{\text{wo-wi}}$	radiation view factor	
g_c	gravitational constant	$Kg \cdot m/N \cdot sec^2$
\bar{h}	average heat transfer coefficient	$W/m^2 \cdot ^\circ K$
K	flow coefficient	
k_{air}	thermal conductivity of air	$W/m \cdot ^\circ K$
k_{ins}	thermal conductivity of insulation	$W/m \cdot ^\circ K$
m	mass flow rate	Kg/sec
Nu_{hd}	local Nusselt number based on hydraulic diameter	
$\overline{Nu}_{\text{hd}}$	average Nusselt number based on hydraulic diameter	
Pr	Prandtl number	
P_{atm}	atmospheric pressure	N/m^2
P_1	pressure upstream of the orifice	N/m^2
P_{wet}	wetted perimeter of the channel	m
Q_{air}	heat convected to the air	W
Q_{li}	heat loss through inner wall insulation	W
Q_{lo}	heat loss through outer wall insulation	W
Q_p	power supplied by the heated plate	W

<u>Symbol</u>	<u>Meaning</u>	<u>Units</u>
Q_r	radiant heat transfer between walls	W
R	gas constant for air	N-m Kg-°K
Re_d	Reynolds number based on channel height	
Re_{hd}	Reynolds number based on hydraulic diameter	
Re_{pipe}	Reynolds number based on pipe diameter	
r_i	radius of curvature of inner curved wall	m
R_{pr}	electrical resistance of precision resistor	Ohms
R_r	total radiation resistance	°K-m ² /W
Ta	Taylor number	
T_{blk}	bulk temperature of flow through the channel	°C
T_{in}	average channel inlet temperature	°C
T_{insi1}	temperature at the plexiglass-insulation interface on the inner surface	°C
T_{insi2}	temperature between the first and second layers of inner insulation	°C
T_{insi3}	temperature between the second and third layers of inner insulation	°C
T_{insol1}	temperature at the plexiglass-insulation interface of the outer surface	°C
T_{insol2}	temperature between the first and second layers of outer insulation	°C
T_{insol3}	temperature between the second and third layers of outer insulation	°C
T_{orf}	air temperature at the orifice	°C
T_{out}	average channel outlet temperature	°C
T_{out}	average channel outlet temperature	°C
T_{wh}	temperature of the heated wall	°C
T_{wi}	average temperature of the lower or convex wall	°C
T_{wo}	average temperature of the upper or concave wall	°C
V_{pr}	voltage drop across the precision resistor	Volts
V_h	voltage drop across the wall heater	Volts
W_{id}	channel width	m
Y	expansion factor	
β	ratio of orifice diameter to pipe diameter	

<u>Symbol</u>	<u>Meaning</u>	<u>Units</u>
ϵ_{cu}	emmissivity of copper	
γ	ratio of specific heats of air	
μ_{air}	dynamic viscosity of air	Kg m-sec
ρ_{air}	density of air	Kg m ³
σ	Stefan-Boltzman constant	W m ² ·°K ⁴
ΔP	pressure drop across the orifice	N m ²
ΔT	average temperature difference of the heated wall and fluid bulk temperature	°C
ΔX_{ins}	insulation layer thickness	m

ACKNOWLEDGEMENTS

The author wishes to express his appreciation to Dr. Matthew D. Kelleher for helping the author to better understand the complexities of heat transfer, and whose patience and guidance were invaluable to the completion of this project.

I. INTRODUCTION

A. BACKGROUND

Lord Rayleigh [Ref. 1] was seemingly the first to investigate the mechanics of flows with curved streamlines. His analysis showed that inviscid curved streamline flows are stable providing that circulation increases with radial distance (for flow between concentric cylinders this condition is met when the outer cylinder spins more quickly than the inner cylinder).

Later, Taylor [Ref. 2] studied viscous flow between concentric rotating cylinders and showed that when the inner cylinder is rotated while holding the outer cylinder stationary, the onset of instability is predicted by the dimensionless parameter:

$$Ta \text{ (Taylor number)} = \frac{Ud}{\nu} \sqrt{\frac{d}{r_i}} \geq 41.3. \quad (\text{eqn 1.1})$$

where U is the tangential velocity of the inner cylinder, d is the gap between cylinders, r_i is the radius of curvature of the inner cylinder, and ν is kinematic viscosity. The instability is manifest in the formation of regularly spaced, counter-rotating vortices whose axes of rotation lie in the circumferential (main flow) direction (see Figure 1.1). Furthermore, Taylor concluded that these vortices form in the laminar flow regime but do *not* induce turbulent main flow [Ref. 3].

The flow of a viscous fluid in a curved channel was studied by Dean [Ref. 4]. He developed an analytical solution for flow in a curved channel approximated by concentric cylinders where the radius of the inner cylinder was much greater than the gap between cylinders. Instead of rotating the inner cylinder Dean imposed a pressure gradient along the channel wall and predicted that flow instability would occur when a critical value of a dimensionless parameter similar to the Taylor number was exceeded:

$$De \text{ (Dean number)} = \frac{Ud}{\nu} \sqrt{\frac{d}{r_i}} \geq 36. \quad (\text{eqn 1.2})$$

where d represents the channel half-width.

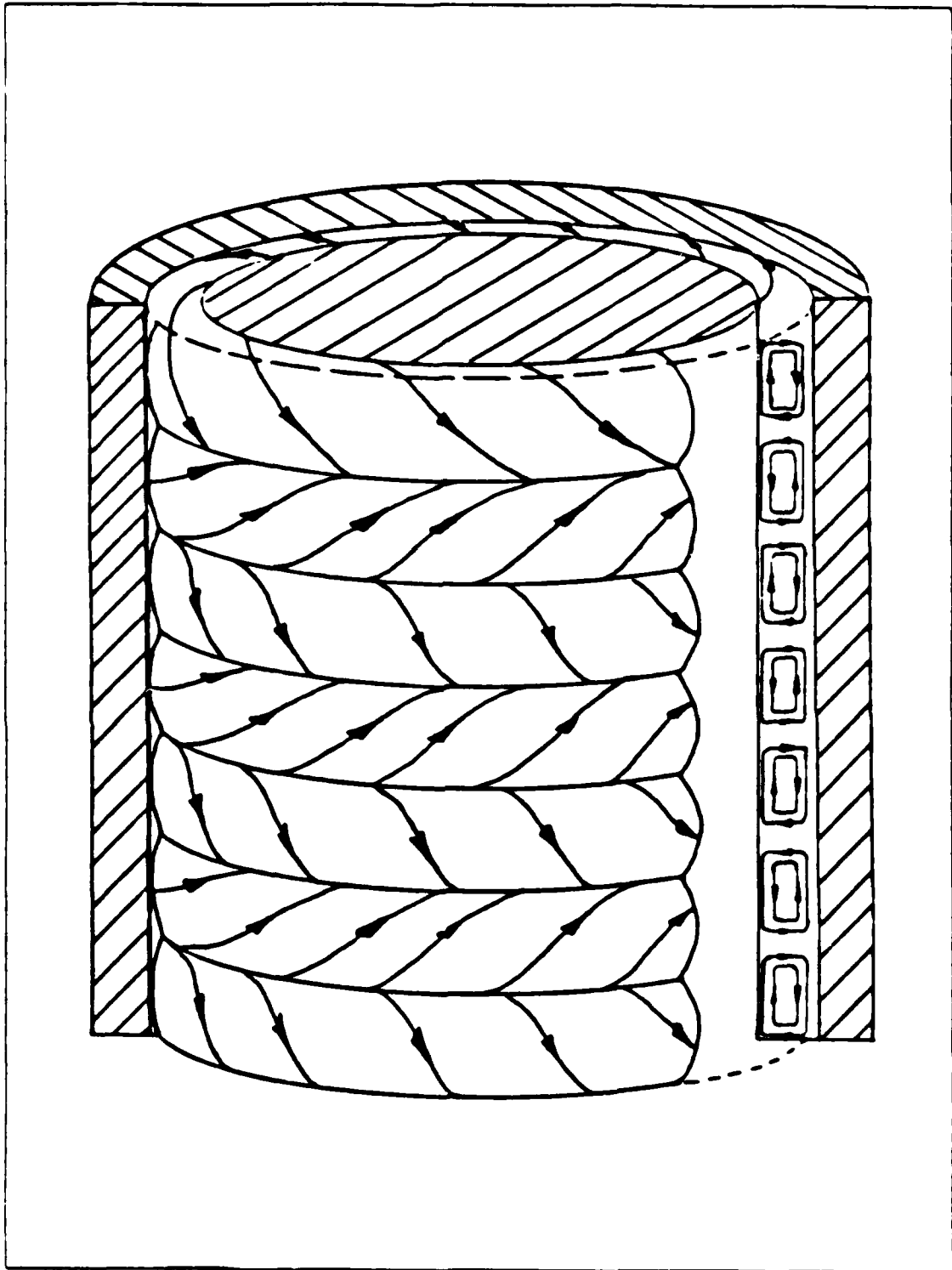


Figure 1.1 Taylor Vortices Between Rotating Cylinders.

Gortler [Ref. 5] went on to investigate viscous flow in a curved channel and concluded that the flow instability predicted by Dean would take a form analogous to the Taylor vortices of concentric cylinder flow (see Figure 1.2). Regularly spaced counter rotating vortices form along axes of rotation parallel to the main flow direction. Yih and Sangster [Ref. 6] concluded that the centrifugal force coupled with the velocity gradient near the concave wall caused instability due to a stratification in specific weight that led to vortex formation.

The secondary flows predicted by Taylor and Gortler (Taylor-Gortler vortices) have been confirmed experimentally using various flow visualization techniques, and hot wire anemometry [Ref. 7]. The presence of these vortices in the laminar flow regime led to speculation of the effect of this secondary flow on heat transfer over curved surfaces. Extensive research has been done which yields good experimental agreement with analytical solutions for laminar flow in curved channels of rectangular cross section [Refs. 8,9,10], and for turbulent flow in a curved rectangular channel of low aspect ratio (ratio of the spanwise dimension to the channel height) [Refs. 11,12,13]. Research in these areas indicates that there is enhancement of heat transfer in these flow regimes when Taylor-Gortler vortices form near the concave wall. However, information relating to the fluid mechanics and heat transfer in the transition and turbulent flow regimes for channels of high aspect ratio is very limited.

B. APPLICATIONS

Studying heat transfer over a curved surface is just one aspect of the complex fluid dynamics and heat transfer problems that exist in an operating gas turbine. The high temperatures characteristic of a combustion engine constrain gas turbine performance because of metallurgical limitations of turbine blades which in turn restricts the efficiency of the turbine. Information gathered in this type of experimentation could lead to a better understanding of the problem and facilitate the design of gas turbines of higher efficiency and power to weight ratio.

C. INTENT OF THIS STUDY

The purpose of this investigation was to study the effect of curvature on heat transfer in a curved rectangular channel of large aspect ratio by gathering extensive

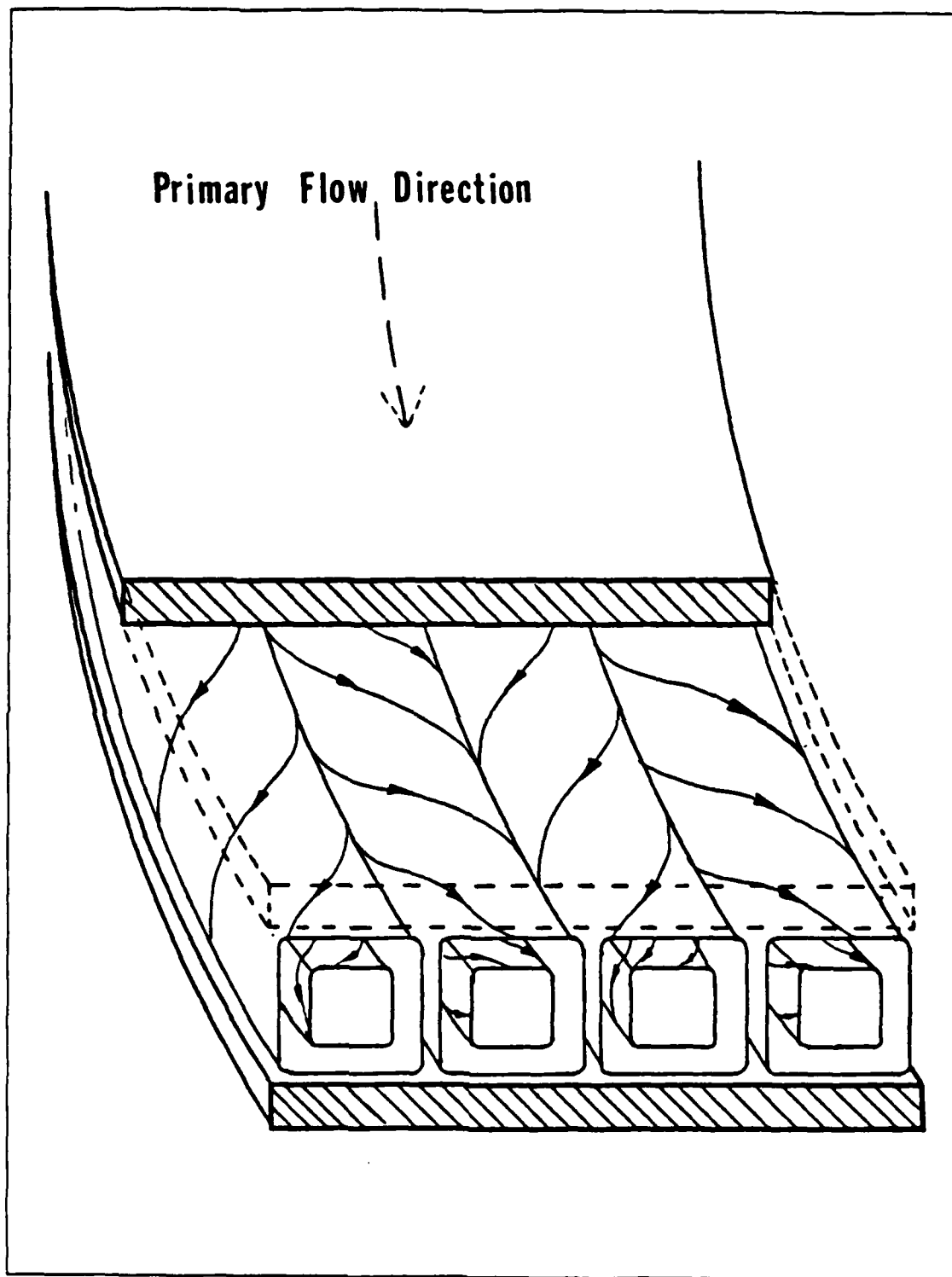


Figure 1.2 Taylor-Gortler Vortices in a Curved Channel.

data relating Nusselt number to Reynolds number for flow over walls of constant heat flux of straight, convex and concave geometry. This information will provide a firm data base for validating computer models of the complex flow and heat transfer in curved rectangular channels similar in geometry.

Data for hydraulically fully developed flow in a straight rectangular channel heated either from above or below was taken to provide a basis for comparison with the flow over a heated convex or concave wall. Empirical correlations similar to the familiar Dittus-Boelter correlation for Nusselt number as a function of Reynolds number were calculated from the data so that the heat transfer enhancement could be described quantitatively and compared to previous data.

A secondary goal was to determine the relative effect of buoyancy on heat transfer in a curved channel. The effect of buoyancy on heat transfer in forced flow must be considered if the effects of free and forced convection are comparable because the combined heat transfer is then dependent on the direction of free convection in comparison to that of forced convection.

II. EXPERIMENTAL APPARATUS AND PROCEDURE

A detailed description of the materials and construction methods used to build the experimental channel and associated instrumentation is contained in G. Galyo's thesis [Ref. 14: pp. 25-43]. Some minor changes had to be made to the existing hardware and computer software and are described herein.

A. DESCRIPTION OF THE APPARATUS

The channel was built of plexiglass, having a channel width of 25.4 cm and a height of 0.635 cm, yielding an aspect ratio of 40:1. The channel was rigidly supported on a wooden frame and insulated over its entire length with three layers of half inch foam insulation. The curved section subtends 180° of arc, and the convex wall (inner curved wall) had a radius of curvature of 29.7 cm (see Figure 2.1). Air was pulled through the channel by a compressor joined to the duct by two inch PVC pipe through a throttle valve.

Four 30.48 cm x 25.4 cm wire wound rubber heaters laminated to copper plates were mounted on the inside walls of the channel to accomplish heating of the air. Two heaters were mounted in the straight test section, one on the upper wall and one on the lower, at a sufficient distance from the channel entrance to insure that flow was hydrodynamically fully developed prior to flowing over the straight heated sections. The two remaining heaters were installed in the curved test section, one on the concave wall and one on the convex wall, with the leading edges of the heaters beginning at an angle of 101.5° from the curved section entrance; this allowed vortices to form prior to flowing over the curved heated sections. The heaters were constant power density type capable of 600 watts each, and could be energized individually or in any combination of pairs by use of two power supplies.

Thirty copper-constantan thermocouples were imbedded in each of the copper plates at the copper plate-rubber heater interface so that local temperatures could be measured (see Figure 2.2). Four thermocouples were mounted laterally across the channel entrance to measure inlet temperature (see Figure 2.1). Similarly, four thermocouples had been mounted at the exit of the channel; however, experimentation

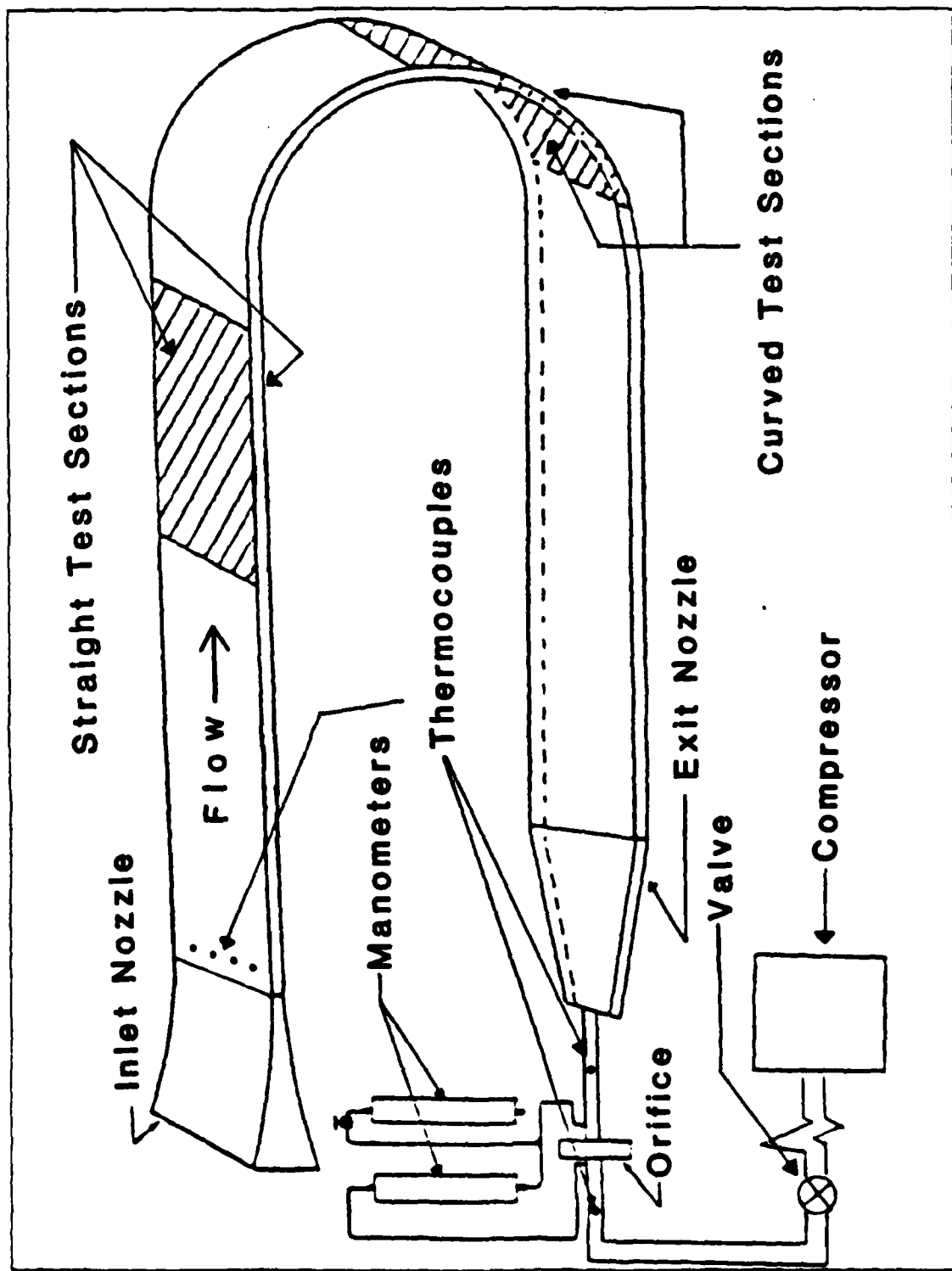


Figure 2.1 Experimental Rectangular Channel.

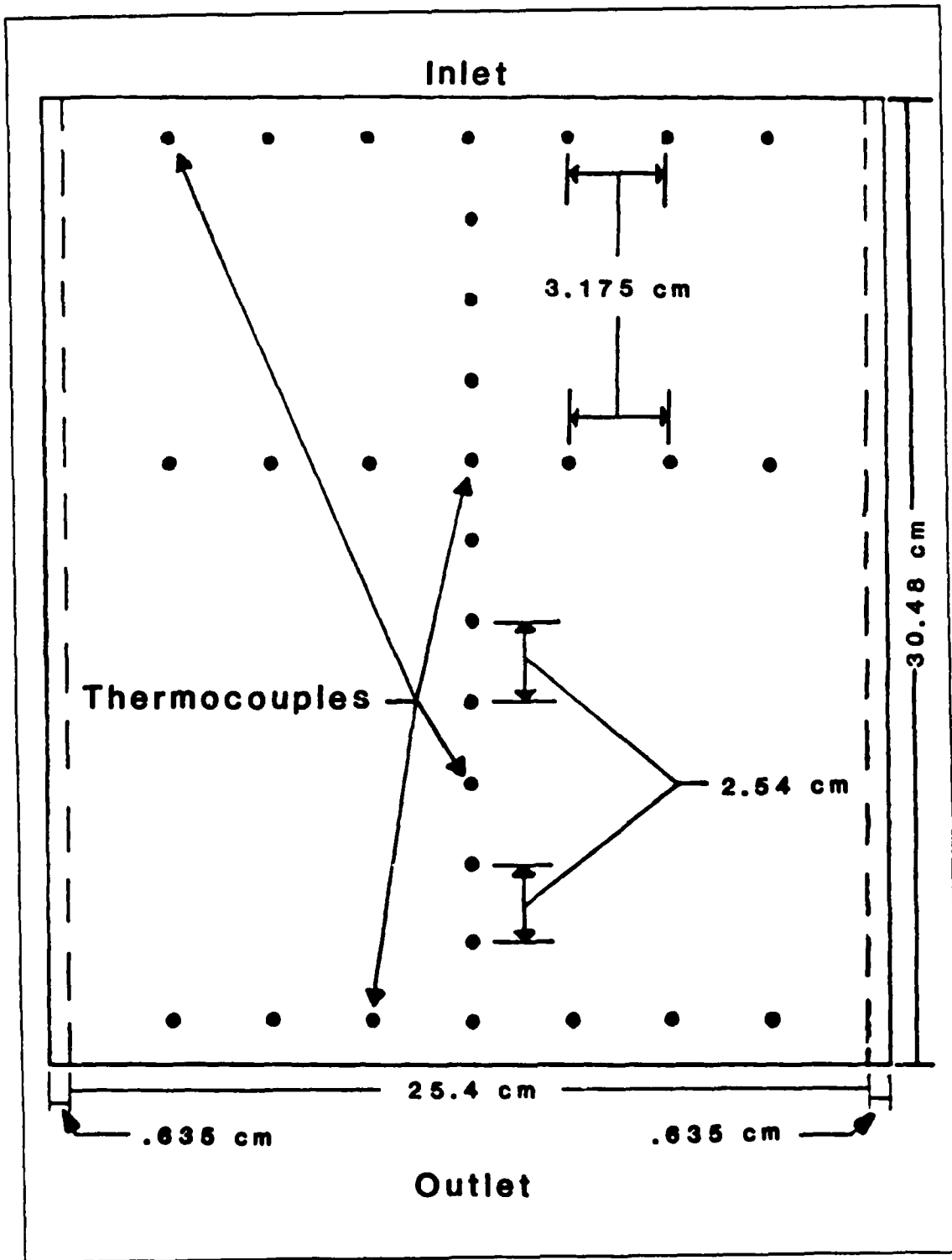


Figure 2.2 Thermocouple Placement in the Heated Plates.

showed that there was insufficient mixing of the air up to the exit which resulted in erratic outlet temperature measurements [Ref. 14: p. 67]. Instead, eighth inch honeycombing was installed at the exit of the channel to promote mixing, and the four exit thermocouples were placed in the PVC pipe near the end of the channel outlet transition bell (see Figure 2.1). Two layers of half inch foam insulation were applied to the PVC to a distance of approximately forty-eight centimeters past these thermocouples to minimize heat loss to the surroundings prior to measuring outlet temperature. One thermocouple was placed downstream of the flow measuring orifice and used to calculate the density of the air flowing through the orifice. Three groups of five thermocouples each were connected in parallel between the layers of insulation surrounding the heated sections so that losses to the surroundings through the insulation could be estimated.

Any combination of eighty voltages from the thermocouples and power supplies could be read by the Hewlett Packard 3054A automatic data acquisition system used for this research. Coupled to the data acquisition system were a Hewlett Packard 9826 computer and a printer which provided control of the data acquisition system and facilitated recording, reducing, and printing of data.

A flow measuring orifice was installed in accordance with the ASME Power Test Code [Ref. 15], and water and mercury manometers were used to measure the pressure upstream of the orifice and differential pressure across the orifice so that mass flowrate could be calculated.

B. EXPERIMENTAL PROCEDURE

The procedures followed for testing were the same irrespective of the specific test configuration. The procedures are:

1. Zero the manometers, shut the system throttle valve, then start the compressor.
2. Use the throttle valve to adjust the differential pressure across the flow measuring orifice to that corresponding to the desired flowrate or Reynolds number. Determining the approximate differential pressure corresponding to a specific Reynolds number takes some experience and the use of the approximation:

$$(\Delta P)_2 \sim \left[\frac{Re_2}{Re_1} \right]^2 (\Delta P)_1 \quad (\text{eqn 2.1})$$

3. Energize the heater and adjust the voltage for the approximate value of $(T_{\text{out}} - T_{\text{in}})$ desired. In these experiments a value of six to twelve degrees centigrade was used for the temperature differential, the objective being to maximize $(T_{\text{out}} - T_{\text{in}})$ while limiting the highest local plate temperature to a maximum of about 100°C. Maximizing this temperature differential lessens the uncertainty of the calculated Nusselt number.
4. Experience showed that the channel reached steady state about four hours after first energizing the heater, and approximately one hour to steady out between consecutive data runs at different flowrates. When all of the following criteria were met, steady state was considered to have been achieved:
 - a. Change in the quantity $(T_{\text{out}} - T_{\text{in}})$ of less than two percent over a ten minute period.
 - b. Change in the heated wall temperature of less than one percent over a ten minute period.
 - c. Change in heated wall insulation temperatures of less than one percent over a ten minute period.
5. When the above criteria for steady state are met, run the data gathering and reducing program (see Appendix A) several times in succession to verify that steady state has been reached. Three to six consecutive data collection runs at steady state meeting the criteria of (4) above are required to determine an average Nusselt number versus Reynolds number relationship. Generally the run-to-run variation in Nusselt number and Reynolds number were much less at lower flowrates.
6. When a sufficient number of consistent data runs have been recorded, throttle to adjust flowrate to the next desired Reynolds number and adjust the heater voltage to achieve the desired plate temperature.

The atmospheric pressure, orifice differential pressure and pressure upstream of the orifice had to be read from a barometer and two manometers and entered into the data reduction program interactively; these parameters were not read by the automatic data acquisition system.

During this study it was noted that small (one degree) ambient temperature perturbations had a noticeable effect on temperatures measured throughout the test system; therefore, close control of ambient temperature oscillations was required so that temperature changes in the test system could be minimized and consistent data measured from run to run.

The initial configuration of the test channel was such that buoyancy induced flow opposed forced flow in the curved test section. After data was taken over the full range of flow that the compressor was capable of, the rig was inverted and data was taken with buoyancy induced flow aiding forced flow. The purpose of this aspect of the study was to determine whether natural convection contributed significantly to the total heat transfer in the curved test sections.

III. DATA REDUCTION

Each heater plate provided a constant surface heat flux. The heater plates were energized by regulated D.C. power supplies through stable precision resistors of low resistance value (see Figure 3.1). The voltage drop across both the heater element and the precision resistor were read and recorded by the data acquisition system. Then the total power supplied by the heater was determined from the relation:

$$Q_p = \frac{V_h \times V_{pr}}{R_{pr}} \quad (\text{eqn 3.1})$$

where R_{pr} was a known value of resistance included as a constant in the data reduction program. The insulated, unheated walls were treated as adiabatic because the heat loss through them was negligible compared to the total heat input from the heater plate. Therefore, the bulk temperature varied linearly from the leading to the trailing edge of the heated plate.

Thermocouple voltages were converted to centigrade temperature using individual thermocouple calibration curves. All temperatures were recorded then combined to calculate specific average temperatures desired.

The actual heat loss to the surroundings was difficult to account for. Typically the estimated total heat loss by conduction through the insulation and by radiation was only about ten percent of the actual total heat loss. The major difficulty in making an accurate prediction of the heat loss was due to not being able to determine the area of the channel over which heat was lost to the surroundings. For the purpose of estimating the heat loss, the area of the heated plate was used as the effective area of loss; however, the plexiglass section of the channel adjacent to the heater plates acts as extended heat transfer surfaces, and the other copper heater surfaces in the channel, which have a low resistance to thermal conduction, act like heat sinks. Therefore, instead of assuming that the energy transferred to the air was equal to the energy input from the plate minus the estimated energy lost to the surroundings over the area of the plate, the energy actually transferred to the working fluid was calculated as follows:

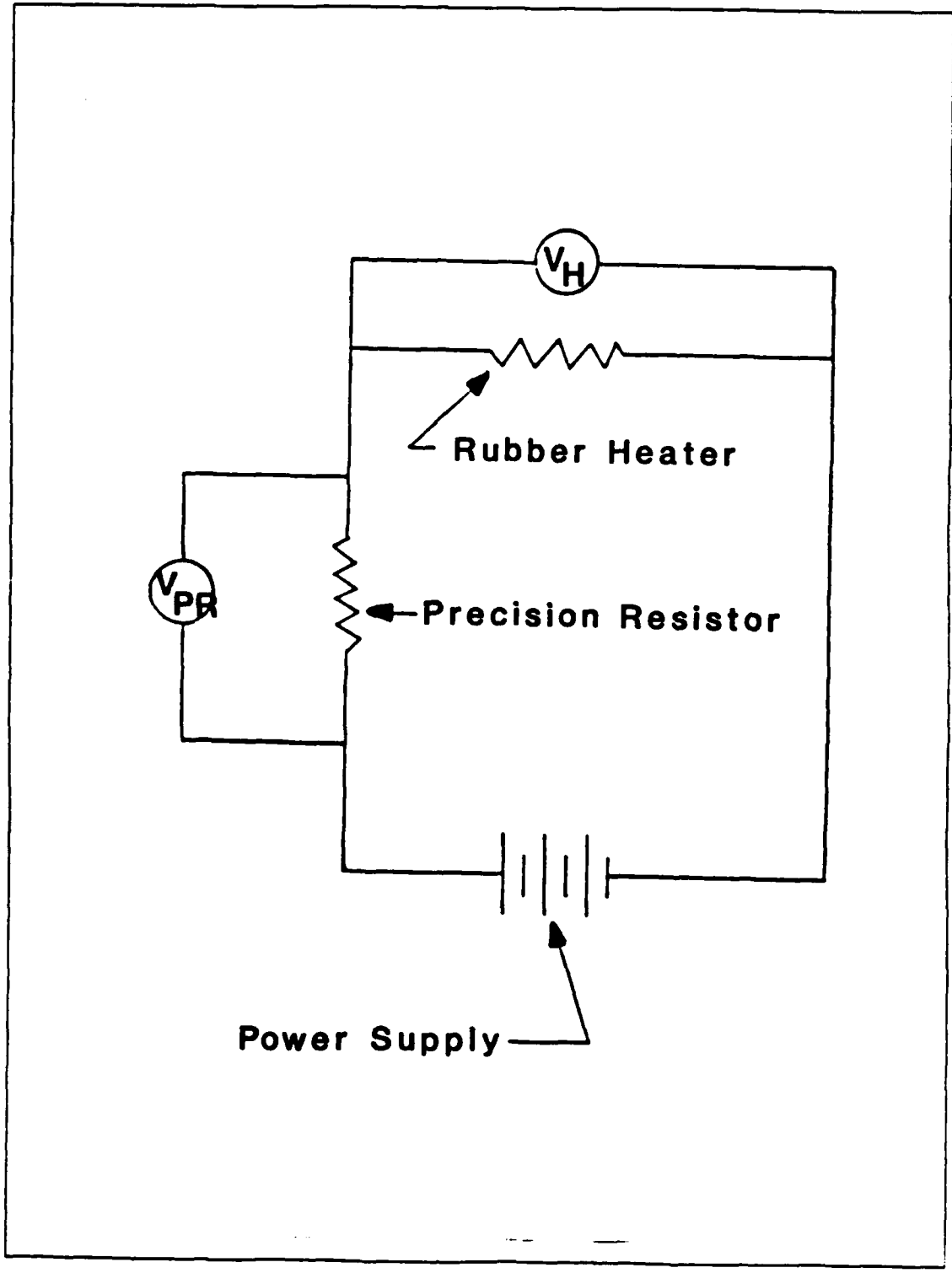


Figure 3.1 Power Measuring Circuit.

$$Q_{\text{air}} = \dot{m}c_p\Delta T \quad (\text{eqn 3.2})$$

where $\Delta T = T_{\text{out}} - T_{\text{in}}$

The corresponding plate average heat transfer coefficient and Nusselt number based on the hydraulic diameter of the duct were then calculated as follows:

$$\bar{h} = \frac{Q_{\text{air}}}{A_{\text{pl}}(T_{\text{wh}} - T_{\text{b}})} \quad (\text{eqn 3.3})$$

$$\text{Nu}_{\text{hd}} = \frac{\bar{h}D_{\text{hd}}}{K_{\text{air}}} \quad (\text{eqn 3.4})$$

where D_{hd} , the hydraulic diameter of the channel, is a geometric constant,

$$D_{\text{hd}} = \frac{4 \times \text{Cross Sectional Area of the Duct}}{\text{Wetted Perimeter of the Duct}} \quad (\text{eqn 3.5})$$

Data on atmospheric pressure, orifice differential pressure, and orifice upstream pressure was used with the flow measuring orifice characteristics and air density based on air temperature at the orifice to calculate mass flowrate, \dot{m} . Reynolds number based on hydraulic diameter was then found by the relation:

$$\text{Re}_{\text{hd}} = \frac{\dot{m}D_{\text{hd}}}{A_c\mu_{\text{air}}} \quad (\text{eqn 3.6})$$

where μ_{air} was the viscosity of the working fluid at the average bulk temperature measured in the test channel. Similarly, Reynolds numbers based on the pipe diameter and channel height were also determined. For the concave and convex sections only, the dimensionless parameter, Dean number, was calculated from:

$$\text{De} = \frac{\dot{m}D_c/2}{A_c\mu_{\text{air}}} \sqrt{\frac{D_c/2}{r_i}} \quad (\text{eqn 3.7})$$

IV. EXPERIMENTAL RESULTS

Several sets of data were taken over the approximate range of Reynolds numbers from 6000 to 20,000. A computer program (see Appendix A) was used to reduce the raw data and calculate the quantities of interest, particularly plate average Nusselt numbers for corresponding Reynolds numbers, both based on the hydraulic diameter of the channel. Three to six separate data sets at each Reynolds number were taken, then averaged to give the value of the quantities of interest.

After extensive data had been taken for the channel configured such that free convection opposed the direction of forced convection, the channel was inverted and several sets of data were taken for the convex and concave plates with the directions of free and forced convection coincident so that the effect of buoyant flow could be determined.

The significant parameters and corresponding uncertainty for the different configurations follows in Tables 1 through 4. Graphic comparisons of plate averaged Nusselt number versus Reynolds number are shown in Figures 4.1 through 4.7. These graphs also include calculated uncertainty ranges for the data, the best fit correlations for each configuration, data for comparison from other sources, and some of the correlations that have been documented in research similiar to this experimentation.

A. HEATING THE STRAIGHT UPPER PLATE

A total of sixty-nine data pairs were taken over an approximate range of Reynolds numbers of 6800 to 20,000 (see Table 1). One means used to analyze the data was the statistics software, MINITAB [Ref. 16]. It was observed that the data at Reynolds numbers below 7000 exhibited a relatively large deviation from the regression in comparison to the data for Reynolds numbers above 7000. This result agrees with previous research done by J. Wilson [Ref. 17: p. 50] which revealed that transition flow in the channel persisted up to a Reynolds number of approximately 7100; therefore, data at Reynolds numbers below 7000 was not included in the regression calculated for the upper straight plate.

Using a least squares regression, a correlation for the heat transfer from the upper plate was determined to be:

$$\overline{Nu}_{hd} = 0.024Re_{hd}^{0.75} \quad (\text{eqn 4.1})$$

where Reynolds and Nusselt numbers are based on the hydraulic diameter. The statistical correlation of the regression was 0.998. The experimental uncertainty of the data was approximately $\pm 5\%$ for Nusselt number and $\pm 6\%$ for Reynolds number.

For comparison, consider the well known Dittus-Boelter correlation based on hydraulic diameter and a Prandtl number of 0.71:

$$\overline{Nu}_{hd} = 0.02Re_{hd}^{0.80} \quad (\text{eqn 4.2})$$

At first glance this small difference between the correlations seems insignificant; however, a look at Figure 4.1 shows that the Dittus-Boelter correlation overestimates the actual Nusselt number by about thirty to thirty-seven percent over its range of applicability ($Re \geq 10,000$).

Also shown for comparison on Figure 4.1 are interpolated values from the Kays and Leung [Ref. 18] analytical solution for infinite parallel plates. These values too lie outside the uncertainty limits of the actual data, but only overestimate Nusselt number by ten to fifteen percent when compared to the finite flat plates of this research.

Data previously taken by G. Galyo [Ref. 14: p. 58] is included in this plot. His data agrees with that of this research to within the bounds of uncertainty. It must be noted that the data taken by Galyo at Reynolds numbers above about 17,000 is less certain than the other data due to the difficulty he encountered in recording an accurate channel outlet temperature at high flowrates [Ref. 14: p. 67].

B. HEATING THE STRAIGHT LOWER PLATE

A total of sixty-four data pairs were recorded over an approximate range of Reynolds numbers of 6000 to 19000 (see Table 2). As in the previous case for the upper plate, the data recorded for Reynolds numbers less than about 7000 were not included in the least squares regression because of their relatively high deviation from the regression. The best fit regression correlation was:

$$\overline{Nu}_{hd} = 0.018Re_{hd}^{0.78} \quad (\text{eqn 4.3})$$

The statistical correlation of the regression was 0.998, and the experimental uncertainty of the data was essentially the same as that for the upper flat plate.

Figure 4.2 shows that over the full range of testing there is essentially no difference in the results for the two flat plate cases. Data previously taken by G. Galyo [Ref. 14: p. 59] is shown as well for comparison, and is well within the experimental uncertainty of the data recorded in this study except at the highest Reynolds number where, as mentioned previously, G. Galyo's data was highly uncertain.

C. HEATING THE OUTER CURVED (CONCAVE) PLATE

Seventy-two data pairs were taken over an approximate range of Reynolds numbers of 6000 to 20,000 (see Table 3). A least squares regression of the data resulted in the relation:

$$\overline{Nu}_{hd} = 0.05Re_{hd}^{0.69} \quad (\text{eqn 4.4})$$

The statistical correlation of the regression was 0.999, and the experimental uncertainty was the same as that for the two previous cases.

Figure 4.3 revealed that the previous data reported by G. Galyo [Ref. 14: p. 60] coincides well with the data recorded in this study except, again, at the highest Reynolds number where G. Galyo had difficulty determining duct outlet temperature accurately. Also shown for comparison are extrapolated correlations from Kreith [Ref. 12: p. 1253], and Brinich and Graham [Ref. 11: p. 35].

In contrast to the results for the flat plates there was no significant deviation from the regression even at the lowest Reynolds number tested for the concave plate. This supports previous research by J. Wilson [Ref. 17: p. 50] which indicated that the limiting Reynolds number for transition flow in curved sections was less than that for flat plates and approximately equal to 5300.

The data for the flat plates was used as a baseline for comparison with the concave plate, and heat transfer enhancement for the concave section was reflected by an increase in Nusselt number of about twenty-one percent at a Reynolds number of 10,000 to fourteen percent at a Reynolds number of 20,000 (see Figure 4.4).

There is a tendency to extrapolate this data to where the correlations for the concave plate and the flat plates converge in order to estimate a Reynolds number where the effect of curvature is no longer significant. For these correlations convergence occurs at a Reynolds number of about 205,000 and a Nusselt number of approximately 232; however, research by Brinich and Graham indicated that the enhancement in heat transfer in a concave section was significant even at Reynolds numbers as high as 250,000.

D. HEATING THE INNER CURVED (CONVEX) PLATE

A total of seventy-three data pairs were recorded over a range of Reynolds numbers of 6000 to 20,000 (see Table 4). A least squares fit of the data gave the relation:

$$\overline{Nu}_{hd} = 0.017Re_{hd}^{0.78} \quad (\text{eqn 4.5})$$

at a statistical correlation of 0.997, and an experimental uncertainty the same as for the previous cases.

Figure 4.5 revealed that, as was the case for the concave plate, there was no significant deviation from the regression even at the lowest Reynolds number tested. A comparison of this data with that reported by G. Galyo [Ref. 14: p. 61] showed that there is agreement to within the bounds of experimental uncertainty except at the highest Reynolds number. For comparison, data reported by Kreith [Ref. 12: p. 1253], and Brinich and Graham [Ref. 11: p. 36] for a convex surface were included in the graph.

Using the flat plate data as a reference of comparison, the reduction in heat transfer on the convex plate was manifest in a Nusselt number consistently six percent lower than that of the flat plates over the entire range of flow rates. This did not represent a large difference between the convex and flat plate cases; however, six

percent was at least one percent more than the conservatively calculated experimental uncertainty of the data. Therefore, this data implied that a decrease in heat transfer on a convex surface should be expected, though probably small.

A comparison of the convex and concave surfaces (see Figure 4.6) pointed out that the concave surface heat transfer is approximately thirty percent greater than that for the convex surface at a Reynolds number of 8000, and about twenty percent greater at a Reynolds number of 20,000.

E. EFFECT OF BUOYANCY

Tables 3 and 4 include data taken when the test channel was oriented such that free convection aided forced convection. Graphical comparison for this case is shown in Figure 4.7.

Data taken for this configuration was within the bounds of experimental uncertainty, and showed no pattern in differing from the case where the direction of free convection opposed that of forced convection. These results indicated that there was no significant buoyant effect over the full range of flow rates studied.

TABLE I
SUMMARY OF STRAIGHT UPPER WALL RESULTS

Re_{hd}	\overline{Nu}_{hd}	$\frac{\delta Re_{hd}}{Re_{hd}}$	$\frac{\delta \overline{Nu}_{hd}}{\overline{Nu}_{hd}}$
6841	17.30	± 0.0560	± 0.0481
7856	19.92		
8588	21.46		
9327	23.06		
10168	24.75	± 0.0576	± 0.0467
10936	26.18		
11947	28.11		
12082	28.38		
12981	29.25		
13969	30.96	± 0.0571	± 0.0485
14997	32.66		
15950	34.62		
17169	36.85		
17839	37.30	± 0.0570	± 0.0495
18927	39.01		
20008	40.27	± 0.0570	± 0.0509

TABLE 2
SUMMARY OF STRAIGHT LOWER WALL RESULTS

Re_{hd}	\overline{Nu}_{hd}	$\frac{\delta Re_{hd}}{Re_{hd}}$	$\frac{\delta \overline{Nu}_{hd}}{\overline{Nu}_{hd}}$
6071	15.03	± 0.0581	± 0.0452
7065	17.85		
8116	19.72	± 0.0573	± 0.0458
8968	21.26		
9997	23.63		
10934	25.35	± 0.0571	± 0.0464
12014	27.17		
12984	29.11		
14047	30.89	± 0.0571	± 0.0473
14989	32.67		
15981	34.10		
16984	35.45	± 0.0570	± 0.0479
18035	36.21		
19002	37.46		
19458	39.83	± 0.0570	± 0.0474

TABLE 3
SUMMARY OF CONCAVE WALL RESULTS

Re_{hd}	\overline{Nu}_{hd}	$\delta Re_{hd} / Re_{hd}$	$\delta \overline{Nu}_{hd} / \overline{Nu}_{hd}$
5884	20.04	± 0.0582	± 0.0448
6025*	19.98*		
7050	22.89		
8016	24.73	± 0.0573	± 0.0450
8044*	24.80*		
9094	26.89		
10025*	28.08*		
10045	28.71		
11023	30.72	± 0.0571	± 0.0451
11977	32.72		
13028	34.90		
13993	36.19	± 0.0571	± 0.0459
14982*	38.05*		
15021	37.95		
15996	40.11		
17053	42.51	± 0.0570	± 0.0464
17943	42.90		
19169	45.26		
20189	46.80	± 0.0571	± 0.0478

* Indicates measurements that were taken with the test channel inverted such that the directions of free and forced convection were coincident.

TABLE 4
SUMMARY OF CONVEX WALL RESULTS

Re_{hd}	\overline{Nu}_{hd}	$\frac{\delta Re_{hd}}{Re_{hd}}$	$\frac{\delta \overline{Nu}_{hd}}{\overline{Nu}_{hd}}$
6065	15.04	± 0.0581	± 0.0492
6088*	15.15*		
7050	16.85		
8009	18.87	± 0.0574	± 0.0498
8034*	18.88*		
9058	19.90		
10020	22.12		
10040*	22.48*		
11054	24.32	± 0.0571	± 0.0525
12003	24.92		
12988	27.83		
13944	29.42	± 0.0571	± 0.0545
14871*	30.57*		
15003	30.72		
15981	32.20		
17009	32.84	± 0.0570	± 0.0517
17898	35.43		
19015	36.25		
20210	37.73	± 0.0571	± 0.0524

* Indicates measurements that were taken with the test channel inverted such that the directions of free and forced convection were coincident.

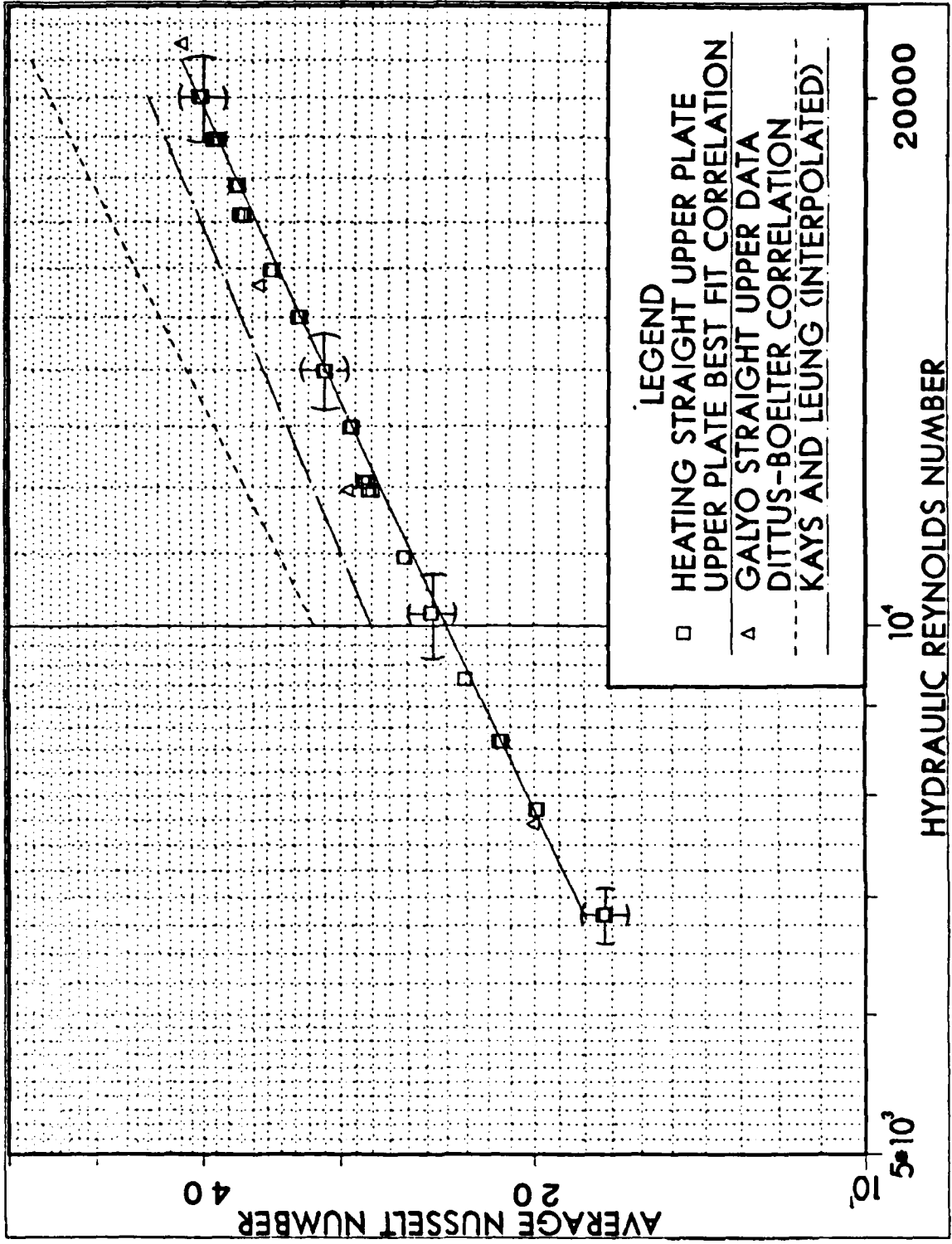


Figure 4.1 Straight Upper Plate Results.

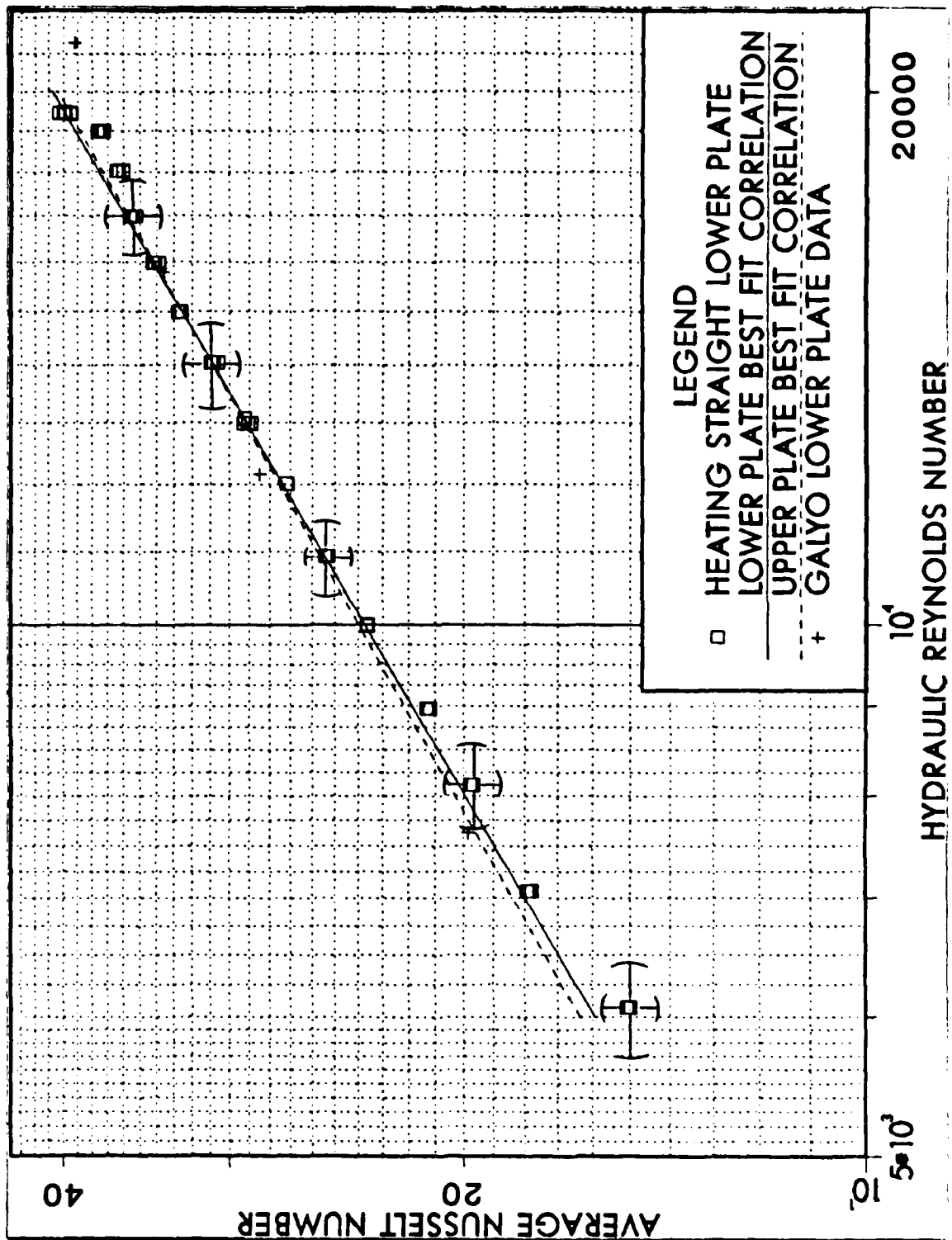


Figure 4.2 Straight Lower Plate Results.

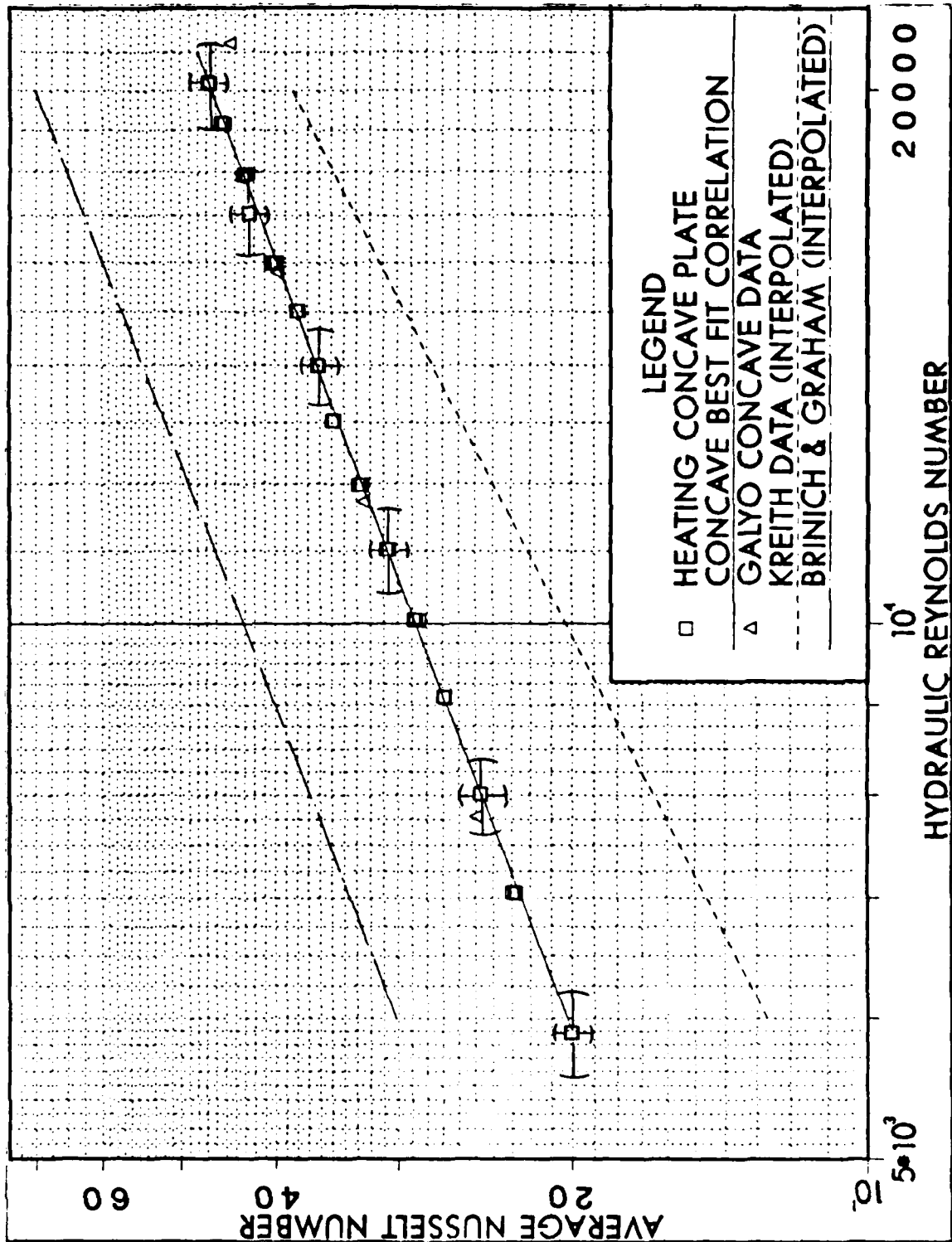


Figure 4.3 Concave Plate Results.

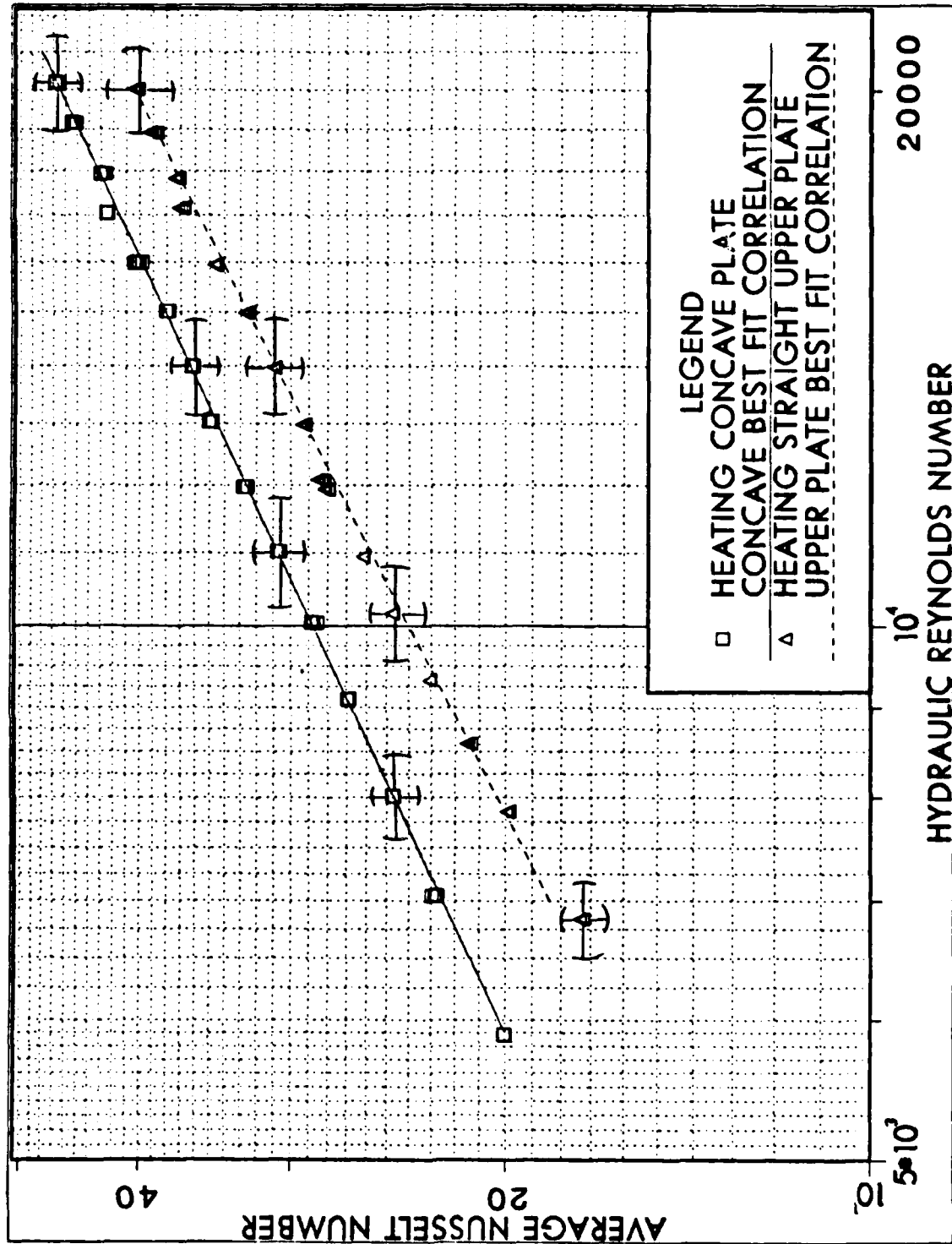


Figure 4.4 Comparison of Straight Upper and Concave Wall Results.

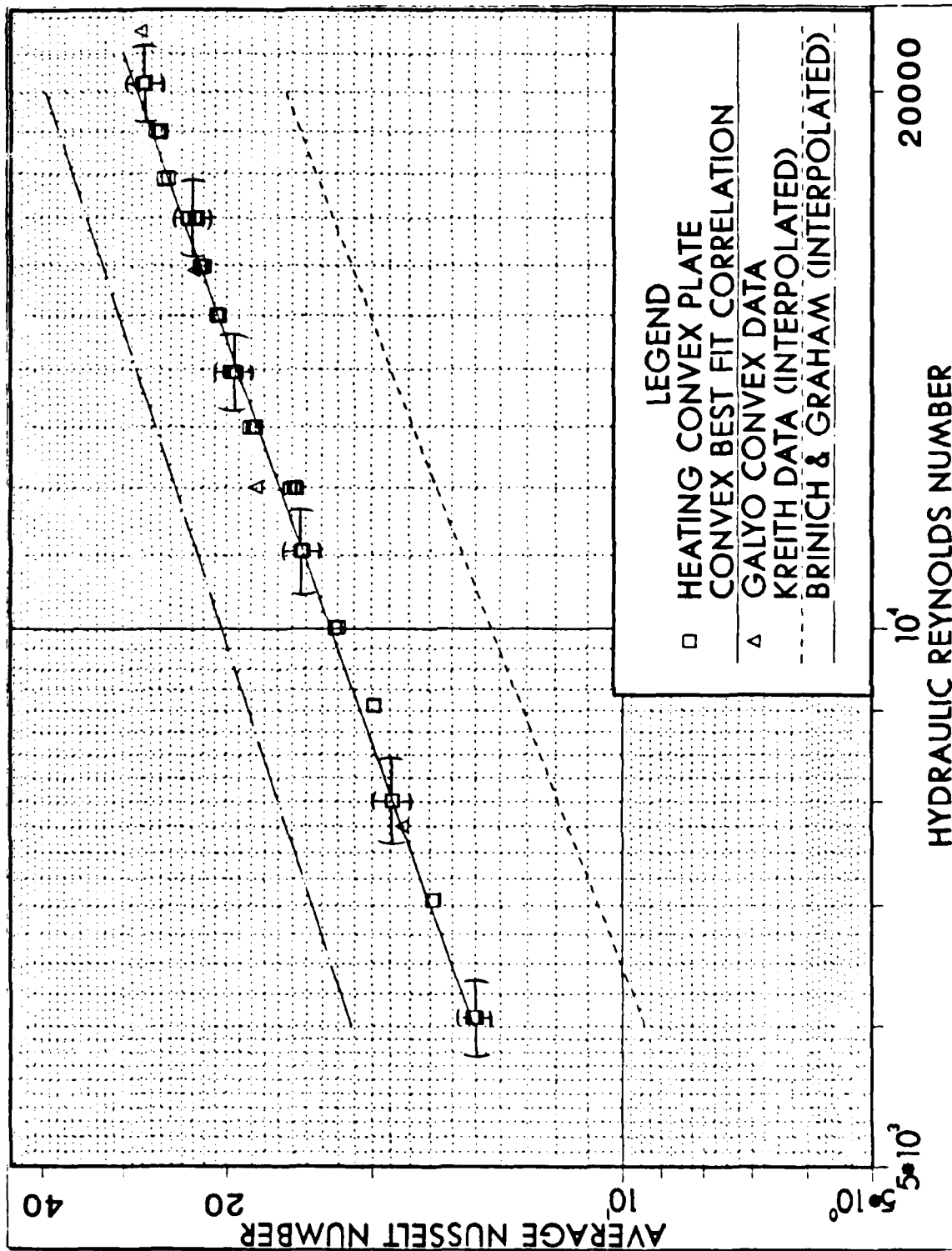


Figure 4.5 Convex Plate Results.

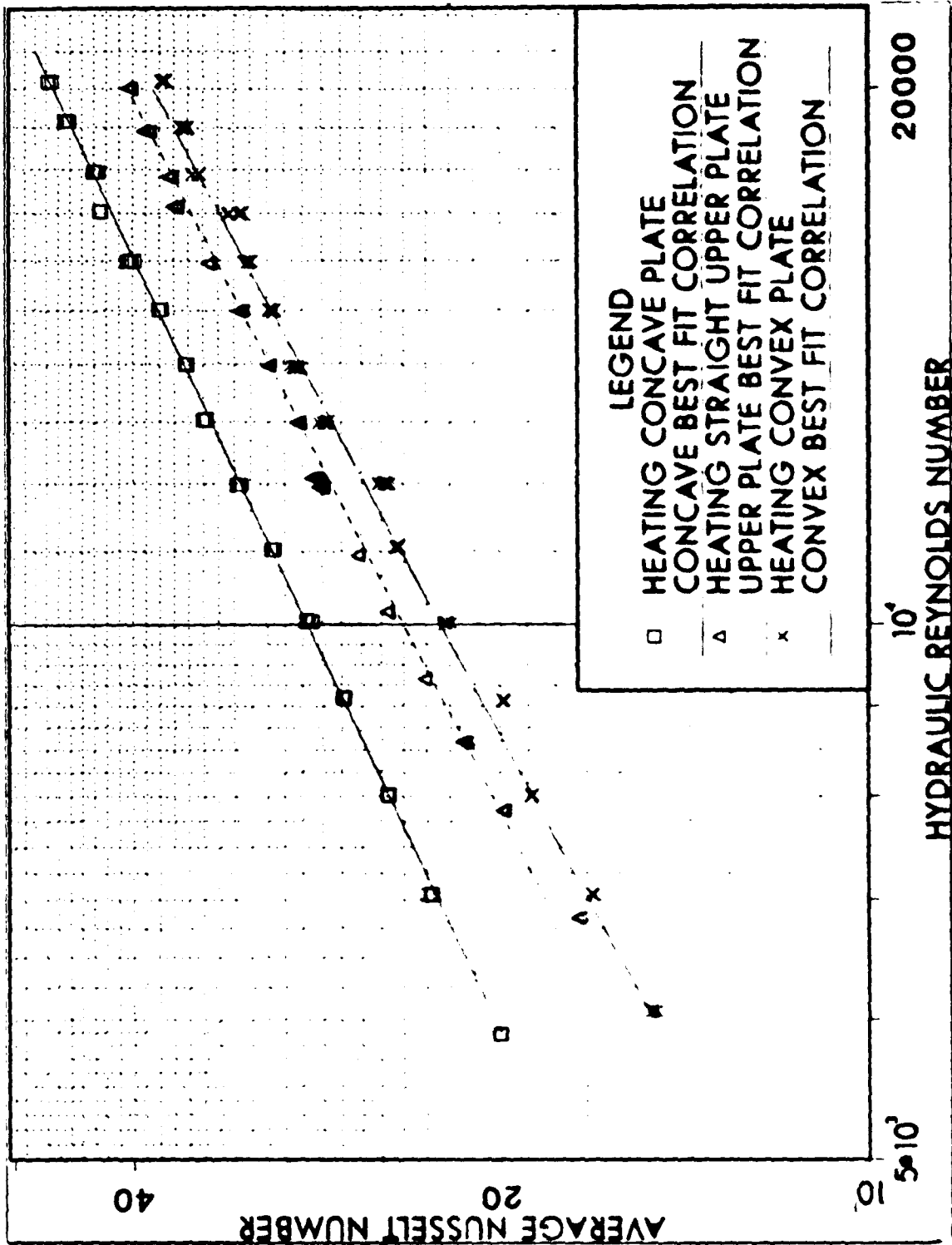


Figure 4.6 Comparison of Concave, Convex and Straight Plate Data.

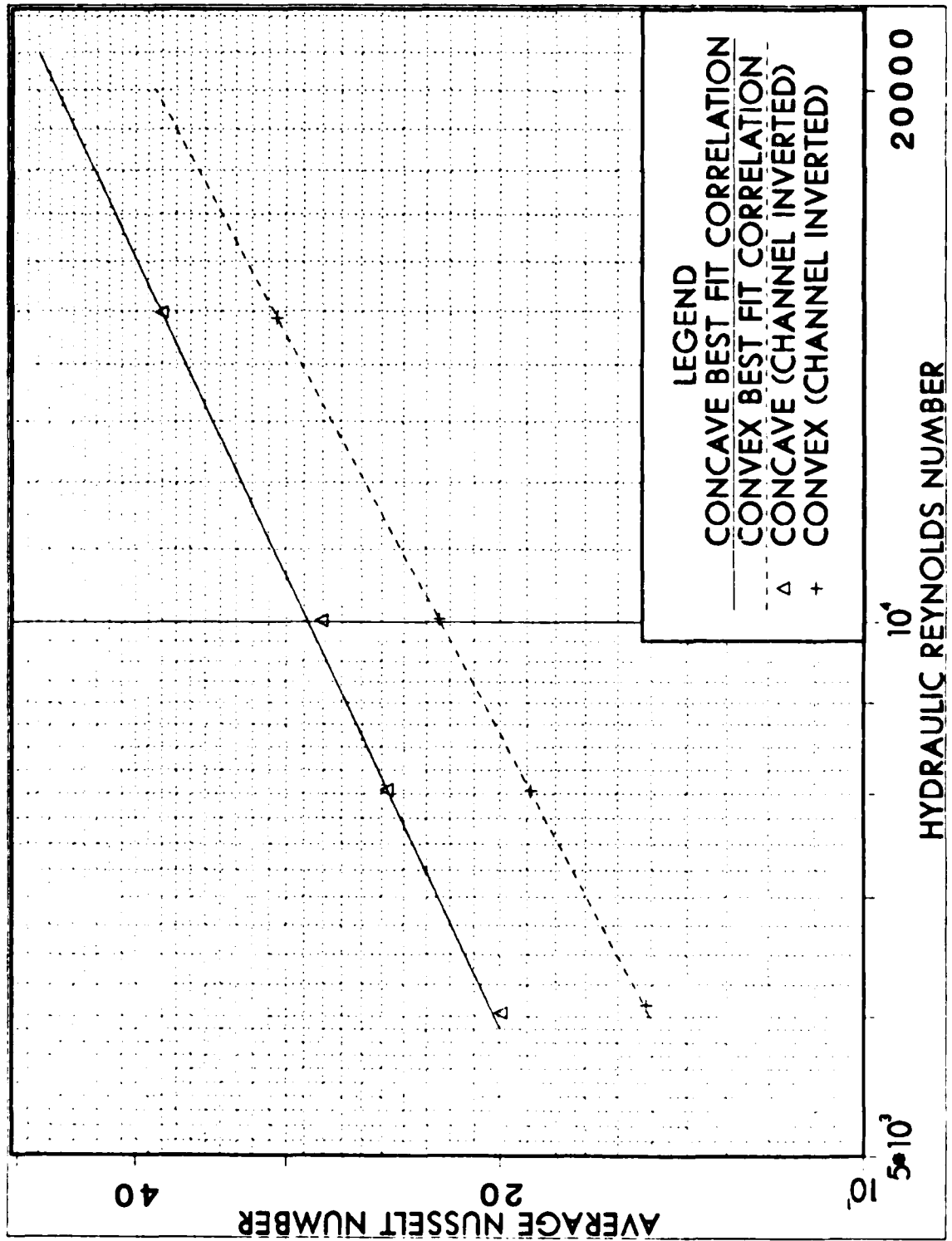


Figure 4.7 Convex Concave Buoyancy Comparison.

V. DISCUSSION

A. FLAT PLATES

The experimental results for the upper and lower straight sections of the channel were essentially the same, and are not considered separately in this discussion.

The Dittus-Boelter correlation for Nusselt number based on the hydraulic diameter of the test channel and a Prandtl number of 0.71 yielded Nusselt numbers thirty to thirty-seven percent higher than those recorded in this experimentation. The Dittus-Boelter correlation is an empirical approximation that was developed to estimate local Nusselt numbers for circular tubes. The correlation itself is only an approximation, and when modified for non-circular ducts where convection coefficients vary about the periphery, the approximation becomes less certain. Here the correlation was used to estimate the average Nusselt number over the length of the heated section. To a first approximation, the Dittus-Boelter correlation can be used to estimate the average Nusselt number because the ratio of the plate length to the hydraulic radius was greater than ten; however, this assumption adds to the uncertainty of the resulting convection coefficient.

The solution for parallel plates of infinite extent developed by Kays and Leung gave Nusselt numbers closer to the experimental results, but was still high by ten to fifteen percent, though ten to fifteen percent accuracy when estimating heat transfer coefficients in the turbulent flow regime is not unusual. Even though the straight section of the test channel approximated flat parallel plates of infinite extent, some sidewall influence on flow was expected and may account for a part of the disparity of the comparison. The graphical comparison shown in Figure 4.1 was developed by linear interpolation of the data from [Ref. 18: p. 552], though there was no evidence to support the assumption that the results of the Kays and Leung solution are a linear function of either Prandtl or Reynolds number; therefore, additional inaccuracy may have been introduced into the comparison.

B. CURVED PLATES

Experimental and analytical investigation of flow and heat transfer on concave and convex surfaces in a rectangular duct of high aspect ratio has thus far received little attention; consequently, there is scant previous work available for comparison. Some results are available for channels of modest aspect ratios, but these do not generally compare well due to the significant sidewall effect introduced at low aspect ratios.

Studies of the flow and heat transfer characteristics in high aspect ratio channels has been done at the Naval Postgraduate School [Refs. 9,14,17,19,20,21,22]. Results of this previous research were comparable to the results of this experimentation and were highly depended upon to validate these results. Only Galyo's work is shown for comparison in this report, but his results agreed within the limits of experimental uncertainty with those of Wilson [Ref. 17], and Daughety [Ref. 22]. The major improvements of this experimentation over that previously done were the decreased experimental uncertainty, especially at the highest Reynolds number, and the preponderance of data that permitted empirical correlations to be determined to a very high level of confidence.

In 1955 Kreith [Ref. 12: p. 1253] investigated the influence of curvature on heat transfer in a rectangular channel of aspect ratio equal to three. For a Prandtl number of 0.71, graphical comparison with the results recorded in this experimentation showed that Kreith's results were approximately thirty percent lower (see Figures 4.3 and 4.5); however, Kreith's test apparatus not only had a much lower aspect ratio, it was also heated by a heating element that was centered between the upper and lower walls of the channel instead of heating the walls themselves.

Research done in 1977 with a channel of aspect ratio six by Brinich and Graham [Ref. 11: pp. 35-36] was shown for comparison in Figures 4.3 and 4.5. The range of Reynolds numbers over which they performed their experiments was approximately 84,000 to 253,000. For the concave surface, Brinich's and Graham's data extrapolated to a Reynolds number of 15,000 yielded a Nusselt number about fifty percent higher than that recorded in this experiment. Likewise, an extrapolation to a Reynolds number of 15,000 for the convex plate showed that there was about a thirty percent difference in the results of the two experiments. These differences are rather large, but,

again, the two studies differed greatly in that the aspect ratios and the range of Reynolds numbers investigated were much different.

Similar research was done in 1978 by Uchida and Koizumi [Ref. 13: pp. 1714-1716], with channels of aspect ratio up to four; however, the full report has not been translated into English. From figures, graphs, and equations included in their report it appears that their test channel was heated along its entire periphery and that the published results were in the form of an average Nusselt number for the combination of a convex and concave wall.

It is unlikely that an average heat transfer coefficient or Nusselt number can be determined when both the convex and concave walls are heated by simple superposition of the individual correlations for the convex and concave walls because of the complex nature of the flow in a curved channel. Therefore, there was no manner in which the results detailed in Ref. 13 could justifiably be compared to the results of this experimentation.

Even though the test equipment was such that a pair of heaters could be energized to supply a constant heat flux on opposite walls of the channel, no conclusive experiments could be performed to determine an average Nusselt number for this configuration.

Referring to (eqn. 3.3) and denoting \bar{h}_1 as the average heat transfer coefficient for single plate heating, and \bar{h}_2 as the average heat transfer coefficient when heating a pair of opposite walls, then:

$$\frac{\bar{h}_1}{\bar{h}_2} = \frac{[(T_{wo} + T_{wi}) 2 - T_{blk}]}{(T_{wh} - T_{blk})} \quad (\text{eqn 5.1})$$

where T_{wh} represents the average temperature when one wall (inner or outer) is heated, and the heat flux from both the inner and outer plates was assumed equal when heating a pair of plates. The average wall temperature term in the numerator of (eqn. 5.1) can be recast as:

$$(T_{wo} + T_{wi}) 2 = T_{wh} + \delta T \quad (\text{eqn 5.2})$$

where δT represents the difference between the average temperature when heating a pair of plates and the single plate average temperature. Combining (eqn. 5.1) and (eqn. 5.2) yields:

$$\begin{aligned} \frac{\bar{h}_1}{\bar{h}_2} &= \frac{(T_{wh} - T_{blk} + \delta T)}{(T_{wh} - T_{blk})} && \text{(eqn 5.3)} \\ &= \frac{1 + \delta T (T_{wh} - T_{blk})}{1} \\ &= \frac{1 + \delta T \Delta T}{1} \end{aligned}$$

(Eqn. 5.3) reveals that only when the temperatures of both plates are the same, such that $\delta T = 0$, when heating a pair of plates, can a true average heat transfer coefficient for both walls be obtained. Strictly speaking the temperature at all corresponding points opposite each other on the plates should be equal to yield an average heat transfer coefficient for the combination of both walls. The heaters used in this experimentation were constant heat flux heaters, and temperatures at corresponding points on opposite walls could not be matched; therefore, conclusive data for the case of heating a pair of plates could not be gathered using the existing equipment.

Though local heat transfer coefficients and Nusselt numbers were calculated at the leading edge, at mid-plate, and at the trailing edge of the heated plates, no conclusive pattern was evident in the data. The same was true for local temperatures. More conclusive results could not be obtained because there were too few thermocouples spaced too far apart; that is, the spanwise thermocouple spacing was greater than the diameter of the Taylor-Gortler vortices that formed.

VI. CONCLUSION

The results of this experimentation, detailed in Chapter IV, indicated that secondary flow in a curved rectangular channel in the form of Taylor-Gortler vortices influenced the heat transfer on the concave and convex surfaces over a range of flow corresponding to Reynolds numbers from about 6000 to 20000.

Correlations of Nusselt number as a function of Reynolds number for the two flat plates, the convex plate, and the concave plate were calculated to a high level of certainty and showed that heat transfer was enhanced by approximately twenty percent on the concave surface as compared to the flat surfaces. Similarly, heat transfer over the convex surface was reduced by approximately six percent in comparison to the flat surfaces. Furthermore, the enhancement or reduction in heat transfer on the curved plates was noted to be greatest at the lowest Reynolds number tested, and tapered off with increased flow rate.

Comparisons made of the results obtained in this experimentation to that of other pertinent research supported the conclusion that heat transfer is enhanced on a concave surface. Experiments performed for the purpose of determining the relative significance of buoyancy induced flow indicated that even at the lowest Reynolds number of 6000, buoyant free convection was negligible compared to forced convection.

VII. RECOMMENDATIONS

A. EQUIPMENT

1. Small oscillations in ambient temperature ($\pm 1^\circ$) noticeably affected temperatures in the channel and contributed to the differences in the results in successive data taking runs. Maintaining close control over ambient temperature would make experimental results more reproducible and decrease the time necessary to gather data.
2. Existing equipment allowed for testing only up to a Reynolds number of about 20000, though the corresponding Reynolds numbers for flow through a gas turbine are much higher. A larger test channel and higher capacity air compressor would be required for experimentation at higher flow rates.
3. A great amount of time was spent waiting approximately four hours for the test channel to reach steady state after first energizing the heater. Installing guard heaters would significantly reduce the warm up time to steady state. Additionally, guard heaters would prevent heat loss through the insulation surrounding the heaters.
4. Pressure sensors that could be read directly by the automatic data acquisition system several times during the course of a data run would increase the accuracy of flow rate measurements and permit successive data runs to be taken without the presence of an operator.
5. More thermocouples should be installed closer together to improve the accuracy of temperature measurements and to facilitate studying the pattern of local variations in temperature and heat transfer in the spanwise and flow-wise directions.
6. The single most significant contributor to experimental uncertainty in the calculated average Nusselt number and hydraulic Reynolds number was the uncertainty in the channel cross section. The uncertainty in experimental results could be greatly reduced if a channel were constructed paying special attention to the cross section dimensions.

B. FURTHER RESEARCH

1. Experimentation similiar to this but at higher flow rates should be done so that a large data base could be established and heat transfer correlations could be calculated for a wide range of application.
2. Experiments at lower flow rates where buoyancy is significant should be done so that a suitable length parameter can be deduced for calculating the Grashof number for curved channel flow.
3. Different curvatures should be studied to determine the effect of the degree of curvature on heat transfer in a curved channel.
4. Thermostatic control should be included in the experimental equipment that could maintain equal plate average temperatures when heating a pair of heaters on opposite walls so that experimental results for channel average heat transfer coefficients could be gathered.

APPENDIX A DATA REDUCTION PROGRAM

```

1000 ! FILE NAME: MAIN
1010 ! LAST REVISION DATE: 19 OCT 1986
1020 ! EDITED BY: LT. J.R. HAWK III
1030!
1040 ! PROGRAM FOR GATHERING AND REDUCING DATA WHEN HEATING ONE COPPER PLATE,
1050 ! WITH 5 MINUTES BETWEEN RUNS. PROGRAM IS MODIFIED TO ACCOUNT FOR
1060 ! BROKEN THERMOCOUPLE CHANNELS 5, 16, 21, AND 26 WHICH EFFECT OUTER
1070 ! CURVED HEATER, THERMOCOUPLE CHANNEL 47 WHICH EFFECTS INNER CURVED
1080 ! HEATER, AND THERMOCOUPLE CHANNEL 11 WHICH EFFECTS OUTER STRAIGHT HEATER
1090!
1100 COM /Co/ D(7),Aa(76,2)
1110 DIM Emf(79),T(79)
1120!
1130 ! CORRELATION FACTORS FOR EMF TO DEGREES CELSIUS FOR CU-CO T/C.
1140!
1150 DATA 0.10086091,25727.94369,-767345.8295,78025595.81
1160 DATA -9247486589,6.97688E+11,-2.66192E+13,3.94078E+14
1170 READ D(*)
1180 PRINTER IS 701
1190 BEEP
1200 INPUT "ENTER MONTH, DAY, AND TIME (MM:DD:HH:MM:SS)",Time$
1210 OUTPUT 709;"TD";Time$
1220 BEEP
1230 INPUT "ENTER INPUT MODE (0-3054A,1-FILE)".In
1240 IF In=1 THEN
1250 BEEP
1260 INPUT "ENTER NAME OF EXISTING DATA FILE",Oldfile$
1270 PRINT USING "20X,""These Results Are From Data File: "",10A";Oldfile$
1280 PRINT
1290 PRINT
1300 ELSE
1310 BEEP
1320 INPUT "ENTER NAME OF NEW DATA FILE?",Newfile$
1330 PRINT USING "20X,""Data For This Run Is Stored In Data File: "",10A";Newf
1340 PRINT
1350 PRINT
1360 END IF
1370!
1380 ! ENTER THE CHANNEL CONFIGURATION.
1390!
1400 PRINT USING "9X,""THE FOLLOWING CHANNEL CONFIGURATION WAS SELECTED:"""
1410 PRINT
1420 BEEP
1430 INPUT "SELECT HEATER TYPE (0-STRAIGHT, 1-CURVED)",Itype
1440 IF Itype=0 THEN PRINT USING "12X,""Heating STRAIGHT Test Section.""
1450 IF Itype=1 THEN PRINT USING "12X,""Heating CURVED Test Section.""
1460 BEEP
1470 INPUT "SELECT HEATER POSITION (0-OUTER, 1-INNER)",Ipos
1480 IF Ipos=0 THEN PRINT USING "12X,""Heating OUTER Plate.""
1490 IF Ipos=1 THEN PRINT USING "12X,""Heating INNER Plate.""
1500 PRINT
1510!

```

```

1520 ! ENTERS FILES WITH T/C CALIBRATION COEFFICIENTS BASED ON HEATER TYPE.
1530!
1540 IF Itype=0 THEN ASSIGN @Filec TO "STRA_COEF"
1550 IF Itype=1 THEN ASSIGN @Filec TO "CURV_COEF"
1560 FOR I=0 TO 76
1570 ENTER @Filec:Aa(I,0),Aa(I,1),Aa(I,2)
1580 NEXT I
1590 ASSIGN @Filec TO *
1600!
1610 ! INSERT DATA STORAGE DISK.
1620!
1630 BEEP
1640 INPUT "CHANGE DISK AND HIT ENTER",Ok
1650 IF Im=1 THEN ASSIGN @File TO Oldfiles$
1660 IF Im=0 THEN
1670 CREATE BDAT Newfile$,40
1680 ASSIGN @File TO Newfiles$
1690 END IF
1700 ENTER 709:Time$
1710 CLEAR 709
1720 PRINT USING "20X, ""Month, Day, and Time: "",14A";Time$
1730 PRINT
1740!
1750 ! FOR DATA RUN READ AND STORE ALL RAW EMF VALUES.
1760!
1770 IF Im=0 THEN
1780 OUTPUT 709:"AR AF00 AL79"
1790 OUTPUT 722:"F1 R1 T1 Z1 FL1"
1800 FOR I=0 TO 79
1810 OUTPUT 709:"AS"
1820 ENTER 722:Emf(I)
1830 NEXT I
1840 OUTPUT @File:Emf(*)
1850 ELSE
1860 ENTER @File:Emf(*)
1870 END IF
1880 OUTPUT 709:"TD"
1890!
1900 ! CONVERT AND CALIBRATE ALL T/C READINGS TO DEGREES CELSIUS.
1910!
1920 PRINT USING "9X, ""THE FOLLOWING DATA WERE RECORDED: ""
1930 PRINT
1940 FOR I=0 TO 79
1950 IF I=38 OR I=39 OR I=77 OR I=78 THEN
1960 IF (Ipos=0 AND I=38) OR (Ipos=1 AND I=77) THEN
1970 Iadd=0
1980 IF Ipos=1 THEN Iadd=39
1990 PRINT USING "12X, ""Heater Voltage (Vh) = "",2D.3D, "" (V) "";Emf(38+Ia
dd)
2000 PRINT USING "12X, ""Resistor Voltage (Vr) = "",2D.3D, "" (V) "";Emf(39+Ia
dd)
2010 IF Ipos=0 THEN PRINT USING "12X, ""Precision Resistor (Rpr) = 2.01729 (Ohm
s) ""
2020 IF Ipos=1 THEN PRINT USING "12X, ""Precision Resistor (Rpr) = 2.00839 (Ohm
s) ""
2030 PRINT
2040 END IF
2050 ELSE
2060!
2070 ! IF T/C OUT OF RANGE PRINT A QUE.
2080!

```

```

2090 Aemf=Emf(I)
2100 IF Aemf<7.09E-4 OR Aemf>3.630E-3 THEN
2110 T(I)=999.99
2120 ELSE
2130 CALL Tvsv(Emf(I),Tt)
2140 IF I=79 THEN
2150 T(I)=Tt
2160 GOTO 2210
2170 END IF
2180 T(I)=FNTcorr(Tt,I)
2190 END IF
2200 END IF
2210 NEXT I
2220!
2230 ! PRINT ALL T/C READINGS.
2240!
2250 PRINT USING "12X,""OUTER PLATE:"""
2260 PRINT USING "14X,""T/C Number:      1      2      3      4      5
6""
2270 PRINT USING "14X,""Temp (C):      ".6(3D.DD,2X)";T(0),T(1),T(2),T(3),T(4),T
(5)
2280 PRINT USING "14X,""T/C Number:      7      8      9      10     11
12""
2290 PRINT USING "14X,""Temp (C):      ".6(3D.DD,2X)";T(6),T(7),T(8),T(9),T(10),
T(11)
2300 PRINT USING "14X,""T/C Number:      13     14     15     16     17
18""
2310 PRINT USING "14X,""Temp (C):      ".6(3D.DD,2X)";T(12),T(13),T(14),T(15),T(
16),T(17)
2320 PRINT USING "14X,""T/C Number:      19     20     21     22     23
24""
2330 PRINT USING "14X,""Temp (C):      ".6(3D.DD,2X)";T(18),T(19),T(20),T(21),T(
22),T(23)
2340 PRINT USING "14X,""T/C Number:      25     26     27     28     29
30""
2350 PRINT USING "14X,""Temp (C):      ".6(3D.DD,2X)";T(24),T(25),T(26),T(27),T(
28),T(29)
2360 PRINT
2370!
2380 ! CALCULATE AVERAGE TEMPERATURE OF OUTER HEATED WALL.
2390!
2400 Sum=0.
2410 IF Itype=0 THEN
2420 FOR I=0 TO 29
2421 IF I=11 THEN 2440
2430 Sum=Sum+T(I)
2440 NEXT I
2450 Two=Sum/29
2460!
2470 ! CORRECTION FOR BROKEN T/C CHANNELS 5, 16, 21, AND 26 IN OUTER CURVED HE
ATER.
2480!
2490 ELSE
2500 FOR I=0 TO 29
2510 IF I=5 OR I=16 OR I=21 OR I=26 THEN 2530
2520 Sum=Sum+T(I)
2530 NEXT I
2540 Two=Sum/26
2550 END IF
2560 PRINT USING "12X,""OUTER INSULATION:"""

```

```

2570 PRINT USING "14X,""T/C Number:   31 (Tinso1)   32 (Tinso2)   33 (Tinso3)"
2580 PRINT USING "14X,""Temp (C):           "",3(3D.DD,8X)";T(30),T(31),T(32)
2590 Tinso1=T(30)
2600 Tinso2=T(31)
2610 Tinso3=T(32)
2620 PRINT
2630 PRINT USING "12X,""ORIFICE TEMP (Torf) = "",3D.DD,"" (C)"";T(33)
2640 PRINT
2650 PRINT USING "12X,""INLET TEMPERATURE:""
2660 PRINT USING "14X,""T/C Number:   35           36           37           38""
2670 PRINT USING "14X,""Temp (C):           "",4(3D.DD,2X)";T(34),T(35),T(36),T(37)
2680 PRINT
2690!
2700 ! CALCULATE AVERAGE INLET TEMPERATURE.
2710!
2720 Sum=0.
2730 FOR I=34 TO 37
2740 Sum=Sum+T(I)
2750 NEXT I
2760 Tin=Sum/4
2770 PRINT USING "12X,""INNER PLATE:""
2780 PRINT USING "14X,""T/C Number:   41           42           43           44           45
46""
2790 PRINT USING "14X,""Temp (C):           "",6(3D.DD,2X)";T(40),T(41),T(42),T(43),T(
44),T(45)
2800 PRINT USING "14X,""T/C Number:   47           48           49           50           51
52""
2810 PRINT USING "14X,""Temp (C):           "",6(3D.DD,2X)";T(46),T(47),T(48),T(49),T(
50),T(51)
2820 PRINT USING "14X,""T/C Number:   53           54           55           56           57
58""
2830 PRINT USING "14X,""Temp (C):           "",6(3D.DD,2X)";T(52),T(53),T(54),T(55),T(
56),T(57)
2840 PRINT USING "14X,""T/C Number:   59           60           61           62           63
64""
2850 PRINT USING "14X,""Temp (C):           "",6(3D.DD,2X)";T(58),T(59),T(60),T(61),T(
62),T(63)
2860 PRINT USING "14X,""T/C Number:   65           66           67           68           69
70""
2870 PRINT USING "14X,""Temp (C):           "",6(3D.DD,2X)";T(64),T(65),T(66),T(67),T(
68),T(69)
2880 PRINT
2890!
2900 ! CALCULATE AVERAGE TEMPERATURE OF INNER HEATED WALL.
2910!
2920 Sum=0.
2930 IF Itype=0 THEN
2940 FOR I=40 TO 69
2950 Sum=Sum+T(I)
2960 NEXT I
2970 Tin=Sum/30
2980!
2990 ! CORRECTION FOR BROKEN T/C CHANNEL 47 IN INNER CURVED HEATER.
3000!
3010 ELSE
3020 FOR I=40 TO 69
3030 IF I=47 THEN 3050
3040 Sum=Sum+T(I)
3050 NEXT I

```

```

3060 Twi=Sum/29
3070 END IF
3080 PRINT USING "12X, ""INNER INSULATION: ""
3090 PRINT USING "14X, ""T/C Number: 71 (Tins1) 72 (Tins2) 73 (Tins3)""
3100 PRINT USING "14X, ""Temp (C): "" ,3(3D,DD,8X)";T(70),T(71),T(72)
3110 Tins1=T(70)
3120 Tins2=T(71)
3130 Tins3=T(72)
3140 PRINT
3150 PRINT USING "12X, ""OUTLET TEMPERATURE: ""
3160 PRINT USING "14X, ""T/C Number: 74 75 76 77""
3170 PRINT USING "14X, ""Temp (C): "" ,4(3D,DD,2X)";T(73),T(74),T(75),T(76)
3180 PRINT USING "0,0"
3190!
3200 ! CALCULATE AVERAGE OUTLET TEMPERATURE.
3210!
3220 Sum=0.
3230 FOR I=73 TO 76
3240 Sum=Sum+T(I)
3250 NEXT I
3260 Tout=Sum/4
3270!
3280 ! CALCULATE DIFFERENCE BETWEEN CHANNEL INLET AND OUTLET TEMPERATURES.
3290!
3300 Tdiff=Tout-Tin
3310!
3320 ! CALCULATE CHANNEL BULK TEMPERATURE.
3330!
3340 Tblk=(Tin+Tout)/2
3350!
3360 ! PRINT CALCULATED TEMPERATURES.
3370!
3380 PRINT USING "9X, ""THE FOLLOWING TEMPERATURES WERE CALCULATED: ""
3390 PRINT
3400 PRINT USING "12X, ""Average Outer Wall Temperature (Two) - "" ,3D,
DD, "" (C)"";Two
3410 PRINT USING "12X, ""Average Inner Wall Temperature (Twi) - "" ,3D,
DD, "" (C)"";Twi
3420 PRINT USING "12X, ""Average Outlet Temperature (Tout) - "" ,3D,
DD, "" (C)"";Tout
3430 PRINT USING "12X, ""Average Inlet Temperature (Tin) - "" ,3D,
DD, "" (C)"";Tin
3440 PRINT USING "12X, ""Channel Inlet and Outlet Temp Diff (Tdiff) - "" ,3D,
DD, "" (C)"";Tdiff
3450 PRINT USING "12X, ""Average Bulk Temperature (Tblk) - "" ,3D,
DD, "" (C)"";Tblk
3460!
3470 ! CALCULATE DELTA T (Tdel) FOR USE IN CALCULATING H LATER.
3480!
3490 Tdelo=Two-Tblk
3500 Tdeli=Twi-Tblk
3510 IF Ipos=0 THEN Tdel=Tdelo
3520 IF Ipos=1 THEN Tdel=Tdeli
3530 PRINT USING "12X, ""Mean Temperature Difference (Tdel) - "" ,3D,
DD, "" (C)"";Tdel
3540!
3550 ! CALCULATE DIFFERENCE BETWEEN OUTER AND INNER WALL.
3560!
3570 Twdiff=ABS(Two-Twi)

```

```

3580 PRINT USING "12X,""Outer and Inner Wall Temp Difference (Tdiff) = ".3D.
DD,"" (C)"";Tdiff
3590!
3600 ! CALCULATE LOCAL CHANNEL TEMPERATURES AT INLET, MIDDLE AND OUTLET.
3610!
3620 Tcin=Tin+(.5*Tdiff/12)
3630 Tcmid=Tin+(4.5*Tdiff/12)
3640 Tcout=Tin+(11.5*Tdiff/12)
3650 PRINT USING "12X,""Average Local Channel Temp at Inlet (Tcin) = ".3D.
DD,"" (C)"";Tcin
3660 PRINT USING "12X,""Average Local Channel Temp at Middle (Tcmid) = ".3D.
DD,"" (C)"";Tcmid
3670 PRINT USING "12X,""Average Local Channel Temp at Outlet (Tcout) = ".3D.
DD,"" (C)"";Tcout
3680!
3690 ! CALCULATE AVERAGE LOCAL HEATED WALL TEMPERATURE AT INLET.
3700!
3710 Sum=0.
3720 Iadd=0
3730 IF Ipos=1 THEN Iadd=40
3740!
3750 ! CORRECTION FOR BROKEN T/C CHANNELS 5, AND 47 CURVED HEATER ONLY.
3760!
3770 IF Itype=1 THEN
3780 FOR I=0 TO 6
3790 IF (Ipos=0 AND I=5) OR (Ipos=1 AND I=6) THEN 3810
3800 Sum=Sum+T(I+Iadd)
3810 NEXT I
3820 Twin=Sum/6
3830 ELSE
3840 FOR I=0 TO 7
3850 IF (Ipos=0 AND I=7) OR (Ipos=1 AND I=6) THEN 3870
3860 Sum=Sum+T(I+Iadd)
3870 NEXT I
3880 Twin=Sum/7
3890 END IF
3900 PRINT USING "12X,""Avg Local Heated Wall Temp at Inlet (Twin) = ".3D.
DD,"" (C)"";Twin
3910!
3920 ! CALCULATE AVERAGE LOCAL HEATED WALL TEMPERATURE NEAR MIDDLE.
3930!
3940 Sum=0.
3950!
3960 ! CORRECTION FOR BROKEN T/C CHANNEL 16 CURVED HEATER ONLY, AND T/C
3961 CHANNEL 11 STRAIGHT HEATER ONLY.
3970!
3980 IF Itype=1 THEN
3990 FOR I=9 TO 16
4000 IF (Ipos=0 AND I=10) OR (Ipos=0 AND I=16) OR (Ipos=1 AND I=9) THEN 4030
4010 Sum=Sum+T(I+Iadd)
4020 NEXT I
4030 IF Ipos=0 THEN Tmid=Sum/6.0
4031 IF Ipos=1 THEN Tmid=Sum/7.0
4040 ELSE
4050 FOR I=9 TO 16
4060 IF (Ipos=0 AND I=10) OR (Ipos=1 AND I=9) OR (Ipos=0 AND I=11) THEN 4080
4070 Sum=Sum+T(I+Iadd)
4080 NEXT I
4081 IF Ipos=0 THEN Tmid=Sum/6.0
4090 IF Ipos=1 THEN Tmid=Sum/7.0

```

```

4100 END IF
4110 PRINT USING "12X," "Avg Local Heated Wall Temp Near Middle (Twmid) = ",3D.
DD," (C)";Twmid
4120!
4130 ! CALCULATE AVERAGE LOCAL HEATED WALL TEMPERATURE AT OUTLET.
4140!
4150 Sum=0.
4160!
4170 ! CORRECTION FOR BROKEN T/C CHANNEL 26 CURVED HEATER ONLY.
4180!
4190 IF Itype=1 AND Ipos=0 THEN
4200 FOR I=23 TO 29
4210 IF I=26 THEN 4230
4220 Sum=Sum+T(I)
4230 NEXT I
4240 Twout=Sum/6
4250 ELSE
4260 FOR I=23 TO 29
4270 Sum=Sum+T(I+Iadd)
4280 NEXT I
4290 Twout=Sum/7
4300 END IF
4310 PRINT USING "12X," "Avg Local Heated Wall Temp at Outlet (Twout) = ",3D.
DD," (C)";Twout
4320 PRINT
4330 PRINT
4340!
4350 ! ENTER ORIFICE PRESSURE DATA.
4360!
4370 BEEP
4380 INPUT "ENTER PATM (inHg), DPM(inH2O), P1M(inH2O), RE1".Patm,Dpm,P1m,Re1
4390 PRINT USING "9X," "THE FOLLOWING ORIFICE DATA WERE ENTERED:"
4400 PRINT
4410 PRINT USING "12X," "Patm(inHg)      DPM(inH2O)      P1M(inH2O)      RE1"
4420 PRINT USING "14X,2(2D.DD,10X),(2D.DD,7X),5D.D";Patm,Dpm,P1m,Re1
4430 PRINT
4440!
4450 ! CONVERT PRESSURE READINGS TO SI UNITS AND P1M TO ABSOLUTE.
4460!
4470 Patm=Patm*3376.8
4480 Pdel=Dpm*248.84
4490 P1=Patm-(P1m*248.84)
4500 Tori=T(33)
4510!
4520 ! PHYSICAL PROPERTIES AND CONSTANTS.
4530!
4540 R=286.987 !FOR AIR.
4550 Rho=P1/(R*(Tori+273.15)) !DENSITY OF AIR AT ORIF PLATE.
4560 Gamma=1.40 !FOR AIR.
4570 Cp=1006 !Cp GOOD FOR blk BETWEEN 12 AND 33 (DEG C).
4580 Gc=1.0
4590 Sigma=5.663E-8
4600 Ecu=.12 !EMISSIVITY OF COPPER.
4610!
4620 ! DIMENSIONS OF CHANNEL.
4630!
4640 Dc=.006350
4650 Wid=.2540
4660 Ri=.297
4670 Pwet=2*(Dc+Wid)
4680 Ac=Dc*Wid

```

```

4690 Dhd=4*Ac/Pwet
4700 Apl=.0774192
4710!
4720 ! PROPERTIES OF INSULATION.
4730!
4740 Xins=.0127
4750 Kins=3.8E-2
4760!
4770 ! ENTER ORIFICE CONFIGURATION.
4780!
4790 BEEP
4800 INPUT "SELECT DIAMETER OF ORIFICE (0=.5334, 1=1.0755 (inches))",Size
4810 IF Size=0 THEN Dorf=.013548
4820 IF Size=1 THEN Dorf=.027318
4830!
4840 ! DIMENSIONS OF PIPE AND ORIFICE PLATE.
4850!
4860 A=(PI*Dorf^2)/4
4870 Dpipe=.051772
4880 Apipe=PI*Dpipe^2/4
4890 Beta=Dorf/Dpipe
4900 PRINT USING "12X,"Dorf(m)          A(m^2)          Beta""
4910 PRINT USING "12X,(Z.6D,6X),(Z.3DE,6X),Z.4D";Dorf,A,Beta
4920 PRINT
4930 PRINT
4940!
4950 ! CORRELATION FOR EXPANSION FACTOR BASED ON 1D AND 1/2D TAPS.
4960!
4970 Y=1-(.41+.35*Beta^4)*(Pdel)/(Gamma*P1)
4980!
4990 ! CALCULATION OF FLOW COEFFICIENT (K) IN SI UNITS.
5000!
5010 B=.0002+2.794E-5/Dpipe+(.0038+1.016E-5/Dpipe)*(Beta^2+(16.5+1.968504E+2*Dp
ipe)*Beta^16)
5020!
5030 ! K1 AND K2 ARE DUMMY VARIABLES TO CALCULATE Ko.
5040!
5050 K1=.6014-5.3974064E-3/Dpipe^.25
5060 K2=(.376+2.8971138E-2/Dpipe^.25)*(1.6129E-7/(Dpipe^2*Beta^2+6.35E-5*Dpipe)
+Beta^4+1.5*Beta^16)
5070 Ko=K1*K2
5080 K=Ko+1000*B/Re1^.5
5090!
5100 ! Mu CORRELATION GOOD FOR Torf BETWEEN 17 AND 41 DEGREES CELSIUS.
5110!
5120 Mu=4.6971429E-8*Torf+1.7194722E-5
5130!
5140 ! CALCULATE Mdot AND REpipe AND COMPARE TO PREDICTED RE1.
5150!
5160 Mdot=K*A*Y*(2*Gc*Rho*Pdel)^(.5)
5170 Repipe=(Mdot*Dpipe)/(Mu*Apipe)
5180 Diff=(ABS(Re1-Repipe)/Re1)*100
5190 Re1=Repipe
5200 IF Diff>.001 THEN 5080
5210 PRINT USING "9X,""THE FOLLOWING DATA WERE CALCULATED:"""
5220 PRINT
5230 PRINT USING "12X,""Orifice Expansion Factor (Y)      = ""Z.4D."";Y
5240 PRINT USING "12X,""Orifice Flow Coefficient (k)     = ""Z.4D."";K
5250 PRINT USING "12X,""Density Based on Torf (Rho)      = ""Z.4D."";Rho (kg/m
3)"";Rho

```

```

5260 PRINT USING "12X,""Viscosity Based on Torf (Mu)   = "",2Z.3DE,"" (kg/m.s)
"";Mu
5270!
5280 ! Mu CORRELATION GOOD FOR Tblk BETWEEN 17 AND 41 DEGREES CELSIUS.
5290!
5300 Mu=4.6971429E-8*Tblk+1.7194722E-5
5310 Red=(Mdot*Dc)/(Mu*Ac)
5320 Rehd=(Mdot*Dhd)/(Mu*Ac)
5330!
5340 ! CALCULATION OF POWER INTO HEATER PLATE.
5350!
5360 Iadd=0
5370 IF Ipos=1 THEN Iadd=39
5380 IF Ipos=0 THEN Rpr=2.01729
5390 IF Ipos=1 THEN Rpr=2.00839
5400 Qp=(Emf(38+Iadd)*Emf(39+Iadd))/Rpr
5410!
5420 ! CALCULATION OF HEAT INPUT TO AIR.
5430!
5440 Qair=Mdot*Cp*(Tout-Tin)
5450!
5460 ! CALCULATE LOCAL HEAT TRANSFER COEF. AND NUSSELT NUMBER.
5470!
5480 Kair=7.7257143E-5*Tcin+.024165836
5490 Hin=Qair/(Apl*(Twin-Tcin))
5500 Nuin=(Hin*Dhd)/Kair
5510 Kair=7.7257143E-5*Tcmid+.024165836
5520 Hmid=Qair/(Apl*(Tmid-Tcmid))
5530 Numid=(Hmid*Dhd)/Kair
5540 Kair=7.7257143E-5*Tcout+.024165836
5550 Hout=Qair/(Apl*(Twout-Tcout))
5560 Nuout=(Hout*Dhd)/Kair
5570!
5580 ! Kair CORRELATION GOOD FOR Tblk BETWEEN 17 AND 41 DEGREES CELSIUS.
5590!
5600 Kair=7.7257143E-5*Tblk+.024165836
5610!
5620 ! CALCULATE AVERAGE HEAT TRANSFER COEF. AND NUSSELT NUMBER.
5630!
5640 Havg=Qair/(Apl*Tdel)
5650 Nuavg=(Havg*Dhd)/Kair
5660!
5670 ! CALCULATE HEAT LOSSES.
5680!
5690 Ql01=(Kins*Apl*(Tins01-Tins02))/Xins
5700 Ql02=(Kins*Apl*(Tins02-Tins03))/Xins
5710 Ql0=(Ql01+Ql02)/2
5720 Ql11=(Kins*Apl*(Tins11-Tins12))/Xins
5730 Ql12=(Kins*Apl*(Tins12-Tins13))/Xins
5740 Ql1=(Ql11+Ql12)/2
5750 Rr=2.0*((1-Ecu)/(Apl*Ecu))+1.0/Apl)
5760 Qr=(Sigma*(ABS((Two+273.15)^4-(Twi+273.15)^4)))/Rr
5770 Qdel=Qp-Qair-Ql01-Qr-Ql11
5780!
5790 ! CALCULATE DEAN NUMBER.
5800!
5810 De=.5*Red*((Dc/2)/R1)^.5
5820 PRINT USING "12X,""Viscosity Based on Tblk (Mu)   = "",2Z.3DE,"" (kg/m.s)
"";Mu
5830 PRINT USING "12X,""Therm Cond Based on Tblk (Kair) = "",Z.3DE,"" (W/m.K)"

```

```

**;Kair
5840 PRINT
5850 PRINT USING "12X,"Patm = "",6D.DD,"" (N/m^2)"";Patm
5860 PRINT USING "12X,"Pdel = "",4D.DD,"" (N/m^2)"";Pdel
5870 PRINT USING "12X,"P1 = "",6D.DD,"" (N/m^2)"";P1
5880 PRINT USING "12X,"Mdot = "",Z.4D,"" (kg/s)"";Mdot
5890 PRINT USING "12X,"Repipe = "",6D.D":Repipe
5900 PRINT USING "12X,"Red = "",6D.D":Red
5910 PRINT USING "12X,"Rehd = "",6D.D":Rehd
5920!
5930 ! ONLY PRINT DEAN NUMBER WHEN HEATING CURVED SECTION.
5940!
5950 IF Itype=1 THEN PRINT USING "12X,"De = "",4D.D":De
5960 PRINT
5970 PRINT USING "12X,"Qp = "",3D.3D,"" (Watts)"";7X,"Qair = "",3D.3D,"" (W
atts)"";Qp,Qair
5980 PRINT USING "12X,"Q1o1 = "",2D.3D,"" (Watts)"";7X,"Q1i1 = "",2D.3D,""
(Watts)"";Q1o1,Q1i1
5990 PRINT USING "12X,"Q1o2 = "",2D.3D,"" (Watts)"";7X,"Q1i2 = "",2D.3D,""
(Watts)"";Q1o2,Q1i2
6000 PRINT USING "12X,"Q1o = "",2D.3D,"" (Watts)"";7X,"Q1i = "",2D.3D,""
(Watts)"";Q1o,Q1i
6010 PRINT USING "12X,"Qr = "",2D.3D,"" (Watts)"";7X,"Qdel = "",2D.3D,""
(Watts)"";Qr,Qdel
6020 PRINT
6030 PRINT USING "12X,"Hin = "",3D.DD,"" (W/m^2C)"";7X,"Nuin = "",3D.DD,"":H
in,Nuin
6040 PRINT USING "12X,"Hmid = "",3D.DD,"" (W/m^2C)"";7X,"Numid = "",3D.DD,"":H
mid,Numid
6050 PRINT USING "12X,"Hout = "",3D.DD,"" (W/m^2C)"";7X,"Nuout = "",3D.DD,"":H
out,Nuout
6060 PRINT USING "12X,"Havg = "",3D.DD,"" (W/m^2C)"";7X,"Nuavg = "",3D.DD,"":H
avg,Nuavg
6070 PRINT
6080 PRINT
6090 BEEP
6100 INPUT "WILL THERE BE ANOTHER RUN? (1-Y,0-N)",Go_on
6110 IF Go_on<>0 THEN
6120 PRINT USING "9,"
6130 IF I=0 THEN WAIT 300
6140 GOTO 1700
6150 END IF
6160 PRINT USING "8X,""END OF RUN""
6170 PRINT USING "9,"
6180 PRINTER IS 1
6190 ASSIGN @File TO *
6200 END
6210!
6220 ! CONVERTS EMF TO DEGREES CELSIUS.
6230!
6240 SUB TvsV(V,T)
6250 COM /Co/ D(7),Aa(76.2)
6260 Sum=0
6270 FOR I=0 TO 7
6280 Sum=Sum+D(I)*V*I
6290 NEXT I
6300 T=Sum
6310 SUBEND
6320!
6330 ! CALIBRATES T/C READINGS.

```

```
6340!  
6350 DEF FNTcorr(T,I)  
6360 COM /Co/ D(7),Aa(76,2)  
6370 Tc=Aa(I,0)  
6380 FOR J=1 TO 2  
6390 Tc=Tc+Aa(I,J)*T*J  
6400 NEXT J  
6410 RETURN Tc  
6420 FNEND
```

APPENDIX B SAMPLE CALCULATION

Figure (B.1) shows the components of the heat balance in the test channel. A sample calculation follows that details the methods used in the data reduction program to estimate the value of the energy balance components and then calculate the hydraulic Reynolds number and average Nusselt number for each data set. A copy of an actual record of one set of experimental data for the concave test section precedes the sample calculations together with a list of the parameters necessary to make the sample calculation.

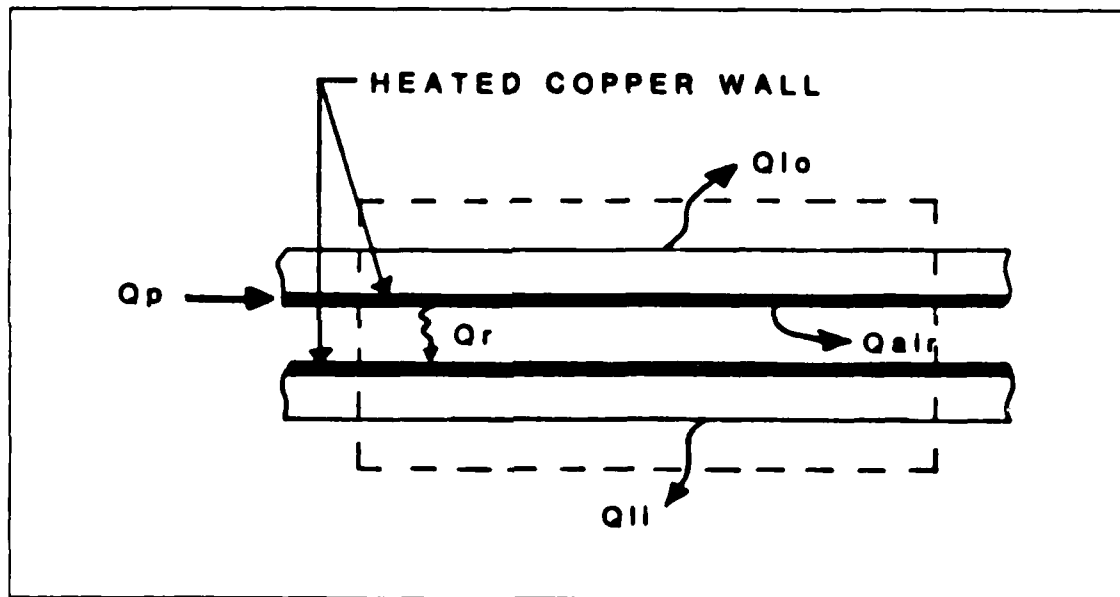


Figure B.1 Test Section Energy Balance.

I. SAMPLE CALCULATION DATA

Month, Day, and Time: 09:16:15:14:54

THE FOLLOWING DATA WERE RECORDED:

Heater Voltage (Vh) = 91.755 (V)
Resistor Voltage (Vr) = 7.704 (V)
Precision Resistor (Rpr) = 2.01729 (Ohms)

OUTER PLATE:

T/C Number:	1	2	3	4	5	6
Temp (C):	72.33	69.67	76.00	68.01	76.20	72.90
T/C Number:	7	8	9	10	11	12
Temp (C):	79.99	72.13	75.77	74.26	77.03	75.00
T/C Number:	13	14	15	16	17	18
Temp (C):	74.32	75.52	75.70	63.57	60.45	78.73
T/C Number:	19	20	21	22	23	24
Temp (C):	79.13	84.26	85.87	69.58	76.27	78.07
T/C Number:	25	26	27	28	29	30
Temp (C):	77.53	80.33	47.70	79.25	80.06	83.47

OUTER INSULATION:

T/C Number:	31 (Tinsol)	32 (Tinsol2)	33 (Tinsol3)
Temp (C):	82.38	56.88	40.01

ORIFICE TEMP (Torf) = 30.25 (C)

INLET TEMPERATURE:

T/C Number:	35	36	37	38
Temp (C):	22.09	22.07	22.08	22.07

INNER PLATE:

T/C Number:	41	42	43	44	45	46
Temp (C):	23.89	23.69	23.40	23.34	23.21	23.49
T/C Number:	47	48	49	50	51	52
Temp (C):	23.28	26.29	23.56	23.27	24.03	24.23
T/C Number:	53	54	55	56	57	58
Temp (C):	23.71	23.82	23.59	23.63	23.56	24.02
T/C Number:	59	60	61	62	63	64
Temp (C):	23.80	24.49	24.27	24.87	24.68	25.87
T/C Number:	65	66	67	68	69	70
Temp (C):	25.56	25.32	25.16	25.04	24.95	24.93

INNER INSULATION:

T/C Number:	71 (Tinsil)	72 (Tinsil2)	73 (Tinsil3)
Temp (C):	24.40	24.13	23.70

OUTLET TEMPERATURE:

T/C Number:	74	75	76	77
Temp (C):	30.66	30.73	30.65	30.69

THE FOLLOWING TEMPERATURES WERE CALCULATED:

Average Outer Wall Temperature (Two)	=	76.46 (C)
Average Inner Wall Temperature (Two)	=	24.16 (C)
Average Outlet Temperature (Tout)	=	30.68 (C)
Average Inlet Temperature (Tin)	=	22.08 (C)
Channel Inlet and Outlet Temp Diff (Tdiff)	=	8.61 (C)
Average Bulk Temperature (Tblk)	=	26.38 (C)
Mean Temperature Difference (Tdel)	=	50.08 (C)
Outer and Inner Wall Temp Difference (Twdiff)	=	52.30 (C)
Average Local Channel Temp at Inlet (Tcin)	=	22.44 (C)
Average Local Channel Temp at Middle (Tcmid)	=	25.30 (C)
Average Local Channel Temp at Outlet (Tcout)	=	30.32 (C)
Avg Local Heated Wall Temp at Inlet (Twin)	=	73.62 (C)
Avg Local Heated Wall Temp Near Middle (Twmid)	=	73.06 (C)
Avg Local Heated Wall Temp at Outlet (Twout)	=	79.78 (C)

THE FOLLOWING ORIFICE DATA WERE ENTERED:

Patm(inHg)	DPM(inH2O)	P1M(inH2O)	RE1
29.86	17.60	16.90	15000.0
Dorf(m)	A(m ²)	Beta	
0.027318	5.861E-04	0.5277	

THE FOLLOWING DATA WERE CALCULATED:

Orifice Expansion Factor (Y)	=	0.9859
Orifice Flow Coefficient (K)	=	0.6326
Density Based on Torf (Rho)	=	1.1099 (kg/m ³)
Viscosity Based on Torf (Mu)	=	18.616E-06 (kg/m.s)
Viscosity Based on Tblk (Mu)	=	18.434E-06 (kg/m.s)
Therm Cond Based on Tblk (Kair)	=	2.620E-02 (W/m.K)

Patm	=	100848.13 (N/m ²)
Pdel	=	4379.58 (N/m ²)
P1	=	96642.74 (N/m ²)
Mdot	=	0.0360 (kg/s)
Repipe	=	47611.8
Red	=	7697.2
Rehd	=	15018.9
De	=	397.9

Qp	=	350.411 (Watts)	Qair	=	311.991 (Watts)
Qlo1	=	5.908 (Watts)	Ql11	=	.063 (Watts)
Qlo2	=	3.908 (Watts)	Ql12	=	.100 (Watts)
Qlo	=	4.308 (Watts)	Ql1	=	.061 (Watts)
Qr	=	1.396 (Watts)	Qdel	=	30.450 (Watts)

Hin	=	78.74 (W/m ² C)	Huin	=	37.67
Hmid	=	84.08 (W/m ² C)	Humid	=	40.00
Hout	=	81.48 (W/m ² C)	Huout	=	38.03
Havg	=	80.47 (W/m ² C)	Huavg	=	38.05

END OF RUN

V_h	= 91.755 V	P_{wet}	= .5207 m
V_{pr}	= 7.704 V	r_i	= .297 m
R_{pr}	= 2.01729 Ω		
P_{atm}	= 29.86 in. Hg		
ΔP	= 17.60 in. H ₂ O		
P_1	= 16.90 in. H ₂ O		
T_{in}	= 22.08 °C		
T_{out}	= 30.68 °C		
T_{wo}	= 76.46 °C		
T_{wi}	= 24.16 °C		
T_{insil}	= 24.40 °C		
T_{insi2}	= 24.13 °C		
T_{insi3}	= 23.70 °C		
T_{insol}	= 82.38 °C		
T_{inso2}	= 56.88 °C		
T_{inso3}	= 40.01 °C		
T_{orf}	= 30.25 °C		
K_{air}	= .0262 W·m ⁻¹ ·K		
c_p	= 1007 J Kg ⁻¹ ·K		
μ_{air}	= $4.6971 \times 10^{-8} \times T_{air} + 1.71947 \times 10^{-5}$ Kg·m ⁻¹ ·s		
K_{ins}	= .0380 W·m ⁻¹ ·°C		
ΔX_{ins}	= .0127 m		
ϵ_{cu}	= 0.12		
σ	= 5.669×10^{-8} W m ⁻² ·°K ⁴		
β	= .5277		
γ	= 1.40		
g_c	= 1.0 Kg·m·N ⁻¹ ·s ²		
R	= 286.98 Nm Kg ⁻¹ ·K		
F_{wo-wi}	= 1.0		
A_{pl}	= .07742 m ²		
A_c	= .0016 m ²		
A_{pipe}	= .00211 m ²		
D_c	= .00635 m		
D_{pipe}	= .0518 m		
D_{orf}	= .027318 m		

2. TEMPERATURE CALCULATIONS

a. Average Temperature of the Outer (Inner) Wall

$$T_{wo}(T_{wi}) = \frac{\sum \text{Outer (Inner) Plate Temperatures}}{\text{Number of Outer (Inner) Plate Thermocouples}} = 76.46^{\circ}\text{C} (24.16^{\circ}\text{C})$$

b. Average Channel Outlet (Inlet) Temperature

$$T_{out}(T_{in}) = \frac{\sum \text{Outlet (Inlet) Temperatures}}{\text{Number of Outlet (Inlet) Thermocouples}} = 30.68^{\circ}\text{C} (22.08^{\circ}\text{C})$$

c. Channel Inlet to Outlet Temperature Difference

$$T_{diff} = T_{out} - T_{in} = 30.68^{\circ}\text{C} - 22.08^{\circ}\text{C} = 8.6^{\circ}\text{C}$$

d. Bulk Temperature of the Flow Through the Channel

$$T_{blk} = \frac{T_{in} + T_{out}}{2.0} = \frac{22.08^{\circ}\text{C} + 30.68^{\circ}\text{C}}{2.0} = 26.38^{\circ}\text{C}$$

e. Average Temperature Difference of the Heated Wall and Fluid Bulk Temperature

$$\Delta T = T_{wo} - T_{blk} = 76.46^{\circ}\text{C} - 26.38^{\circ}\text{C} = 50.08^{\circ}\text{C}$$

f. Temperature Difference Between the Outer and Inner Walls

$$T_{wdiff} = T_{wo} - T_{wi} = 76.46^{\circ}\text{C} - 24.16^{\circ}\text{C} = 52.30^{\circ}\text{C}$$

3. POWER CALCULATIONS

a. Power supplied by the Heated Plate

$$Q_p = \frac{V_h \times V_{pr}}{R_{pr}} = \frac{91.755\text{V} \times 7.704\text{V}}{2.01729\Omega} = 350.41 \text{ Watts}$$

b. Power Loss Through the Outer Wall Insulation

$$\begin{aligned} Q_{lo} &= (1/2)(Q_{lo1} + Q_{lo2}) \\ &= (1/2)\left[\left(\frac{T_{inso1} - T_{inso2}}{\Delta X_{ins}}\right)k_{ins}A_{pl} \right. \\ &\quad \left. + \left(\frac{T_{inso2} - T_{inso3}}{\Delta X_{ins}}\right)k_{ins}A_{pl}\right] = \\ &= (1/2)(.07742\text{m}^2) \frac{(0.038 \text{ W m}^\circ\text{C})}{.0127\text{m}} [(82.38 - 56.88(^\circ\text{C})) + (56.88 - 40.01(^\circ\text{C}))] = 4.908\text{W} \end{aligned}$$

c. Power Loss Through the Inner Wall Insulation

$$\begin{aligned} Q_{li} &= (1/2)(Q_{li1} + Q_{li2}) \\ &= (1/2)\left[\left(\frac{T_{insi1} - T_{insi2}}{\Delta X_{ins}}\right)k_{ins}A_{pl} \right. \\ &\quad \left. + \left(\frac{T_{insi2} - T_{insi3}}{\Delta X_{ins}}\right)k_{ins}A_{pl}\right] = \\ &= (1/2)(.07742\text{m}^2) \frac{(0.038 \text{ W m}^\circ\text{C})}{.0127\text{m}} [(24.40 - 24.13(^\circ\text{C})) + (24.13 - 23.70(^\circ\text{C}))] = .081\text{W} \end{aligned}$$

d. Heat Loss by Radiation

1. Radiation Resistance

$$\begin{aligned} R_r &= 2 \times \left(\frac{1 - \epsilon_{cu}}{A_{pl} \times \epsilon_{cu}}\right) + \frac{1}{A_{pl} \times F_{wo\ wi}} = \\ &= \frac{1}{A_{pl}} \left(\frac{2}{\epsilon_{cu}} - 1\right) = \frac{1}{0.07742\text{m}^2} \left(\frac{2}{0.12} - 1\right) = 202.36 \text{ m}^2 \end{aligned}$$

2. Heat Radiated

$$\begin{aligned} Q_r &= \frac{\sigma(T_{wo}^4 - T_{wi}^4)}{R_r} \\ &= \frac{(5.669 \times 10^{-8})[(76.46 + 273)^4 - (24.16 + 273)^4]}{202.36} = 1.996 \text{ W} \end{aligned}$$

4. MASS FLOW RATE CALCULATIONS

a. Pressure Conversions

$$P_{\text{atm}} = 29.865 \text{ in Hg} \times 3376.8 = 100848.13 \text{ N m}^2$$

$$\Delta P = 17.60 \text{ in H}_2\text{O} \times 248.84 = 4379.58 \text{ N m}^2$$

$$P_1 = (16.90 \text{ in H}_2\text{O} \times 248.84) - 100848.13 = 96642.74 \text{ N m}^2$$

b. Density of Air

$$\rho_{\text{air}} = \frac{P_1}{RT_{\text{orf}}} = \frac{(96642.74)}{(286.98)(30.25 + 273)} = 1.1099 \text{ Kg m}^3$$

c. Expansion Factor

$$Y = 1 - (0.41 + 0.35\beta^4) \frac{\Delta P}{\gamma P_1}$$
$$= 1 - [0.41 + 0.35(0.5277)^4] \frac{4379.58}{(1.40)(96642.74)} = 0.9859$$

d. Mass Flow Rate

$$\dot{m} = YKA \sqrt{2g_c \rho_{\text{air}} \Delta P} = (.9859)K(.0005861 \text{ m}^2)$$
$$\times \sqrt{2(1 \text{ Kg-m N s}^2)(1.1099 \text{ Kg m}^3)(4379.58 \text{ N m}^2)} = .05669K \text{ Kg s}$$

Iterate to find \dot{m} :

Assume a hydraulic Reynolds number = 15000

$$Re_{\text{pipe}} \sim \left(\frac{D_{\text{pipe}} A_c}{D_{\text{hd}} A_{\text{pipe}}} \right) Re_{\text{hd}} = \left(\frac{.0518 \times .0016}{.01229 \times .00211} \right) \sim 3.1961 \times Re_{\text{hd}}$$

$$\rightarrow Re_{\text{pipe}} \sim 15000(3.1961) = 47942$$

Interpolate in the appropriate table in Reference 15 for K, the flow coefficient:

$$K = .6329$$

(Note that the computer program used to reduce the data used an approximate polynomial to find the correct value of the flow coefficient, K.)

$$\rightarrow \dot{m} = (.05669)(.6329) = .0359 \text{ Kg s}$$

Solve for the improved value of Re_{pipe} :

$$Re_{\text{pipe}} = \frac{\dot{m} D_{\text{pipe}}}{A_{\text{pipe}} \mu_{\text{air}}} = \frac{(.0359)(.0518)}{(.00211)(18.616 \times 10^{-4})} = 47315$$

Iterate until successive values of \dot{m} differ by less than .001: $\dot{m} = .0360$

5. REYNOLDS NUMBER CALCULATIONS

a. Re Based on Pipe Diameter

$$Re_{\text{pipe}} = \frac{\dot{m} D_{\text{pipe}}}{A_{\text{pipe}} \mu_{\text{air}}} = \frac{(.0360)(.0518)}{(.00211)(18.616 \times 10^{-6})} = 47475$$

b. Re Based on Channel Height

$$Re_d = \frac{\dot{m} D_c}{A_c \mu_{\text{air}}} = \frac{(.0360)(.00635)}{(.0016)(18.434 \times 10^{-6})} = 7751$$

c. Re Based on Hydraulic Diameter of the Channel

$$Re_{\text{hd}} = \frac{\dot{m} D_{\text{hd}}}{A_c \mu_{\text{air}}} = \frac{(.0360)(.01229)}{(.0016)(18.434 \times 10^{-6})} = 15000.8$$

6. HEAT TRANSFERRED TO THE WORKING FLUID

$$Q_{\text{air}} = \dot{m} c_p (T_{\text{out}} - T_{\text{in}}) = (.0360 \text{ Kg s})(1007 \text{ J Kg}^{-1}\text{C}^{-1})(30.86 - 22.08)^{\circ}\text{C} = 312 \text{ W}$$

7. AVERAGE HEAT TRANSFER COEFFICIENT CALCULATION

$$\bar{h} = \frac{Q_{\text{air}}}{A_{\text{pl}} \Delta T} = \frac{312 \text{ W}}{(.07742 \text{ m}^2)(50.08^{\circ}\text{C})} = 80.5 \text{ W m}^{-2}\text{C}^{-1}$$

8. AVERAGE NUSSLELT NUMBER CALCULATION

$$\overline{Nu}_{\text{hd}} = \frac{\bar{h} D_{\text{hd}}}{K_{\text{air}}} = \frac{(80.5 \text{ W m}^{-2}\text{C}^{-1})(.01229 \text{ m}^2)}{.0262 \text{ W m}^{-1}\text{C}^{-1}} = 37.8$$

9. DEAN NUMBER CALCULATION

$$De = \frac{Re_d}{2} = \frac{\sqrt{\frac{D_c}{r_i}}}{2} = \frac{7751}{2} \sqrt{\frac{.00635^2}{.297}} = 400.7$$

APPENDIX C EXPERIMENTAL UNCERTAINTY

The experimental uncertainty in calculated parameters was determined in accordance with the method described by Kline and McClintock [Ref. 23]

The qualitative results shown here correspond to the data set and calculation of Appendix B. There was a significant decrease in the experimental uncertainty of the average Nusselt number for Reynolds numbers above 17,000 in this experimentation compared to that of Galyo [Ref. 14: pp. 104-105] because of the changes made to the test channel that promoted mixing of the working fluid at the exit of the channel.

The equations used to determine the experimental uncertainty of calculated parameters are shown below.

1. DENSITY OF THE WORKING FLUID

$$\frac{\delta \rho}{\rho} = \left[\left(\frac{\delta R}{R} \right)^2 + \left(\frac{\delta P_1}{P_1} \right)^2 + \left(\frac{\delta T_{orf}}{T_{orf}} \right)^2 \right]^{0.5}$$

2. MASS FLOW RATE OF THE WORKING FLUID

$$\frac{\delta \dot{m}}{\dot{m}} = \left[\left(\frac{\delta Y}{Y} \right)^2 + \left(\frac{\delta K}{K} \right)^2 + \left(\frac{\delta A}{A} \right)^2 \right] + (1.4) \left[\left(\frac{\delta \rho_{air}}{\rho_{air}} \right)^2 + \left(\frac{\delta \Delta P}{\Delta P} \right)^2 \right]^{0.5}$$

3. HEAT TRANSFERRED TO THE WORKING FLUID

$$\frac{\delta Q_{air}}{Q_{air}} = \left[\left(\frac{\delta \dot{m}}{\dot{m}} \right)^2 + \left(\frac{\delta c_p}{c_p} \right)^2 + \left(\frac{\delta(T_{out} - T_{in})}{(T_{out} - T_{in})} \right)^2 \right]^{0.5}$$

4. AVERAGE HEAT TRANSFER COEFFICIENT

$$\frac{\delta \bar{h}}{\bar{h}} = \left[\left(\frac{\delta Q_{air}}{Q_{air}} \right)^2 + \left(\frac{\delta A_{pl}}{A_{pl}} \right)^2 + \left(\frac{\delta \Delta T}{\Delta T} \right)^2 \right]^{0.5}$$

5. AVERAGE NUSSELT NUMBER

$$\frac{\delta \overline{Nu}_{hd}}{\overline{Nu}_{hd}} = \left[\left(\frac{\delta \bar{h}}{\bar{h}} \right)^2 + \left(\frac{\delta D_{hd}}{D_{hd}} \right)^2 + \left(\frac{\delta K_{air}}{K_{air}} \right)^2 \right]^{0.5}$$

6. HYDRAULIC REYNOLDS NUMBER

$$\frac{\delta Re}{Re} = \left[\left(\frac{\delta \dot{m}}{\dot{m}} \right)^2 + \left(\frac{\delta D_{hd}}{D_{hd}} \right)^2 + \left(\frac{\delta \mu_{air}}{\mu_{air}} \right)^2 + \left(\frac{\delta A_c}{A_c} \right)^2 \right]^{0.5}$$

Several parameters used in the calculations described herein had uncertainties that were constant over the entire range of testing. These quantities and their relative uncertainties follow:

Quantity (B)	Uncertainty ($\pm \delta B$)
A	.0020
A _c	.0408
A _{pl}	.0006
c _p	.0020
D _c	.0400
D _{hd}	.0391
K	.0030
K _{air}	.0038
P _{atm}	.0010
R	.0003
W _{id}	.0080
Y	.0020
μ _{air}	.0054

The approximating polynomials used to resolve thermocouple voltages into temperatures matched actual temperatures to within less than $\pm 0.1^\circ\text{C}$ over a range of temperatures from 20°C to 85°C ; however, in some cases this temperature range was exceeded. A conservative estimate of the uncertainty of temperatures measured by thermocouples was set at $\pm 0.1^\circ\text{C}$, the accuracy of the thermocouples specified by the manufacturer of the thermocouple wire. The following uncertainties were used in calculations:

Quantity (T)	Uncertainty ($\pm T$)
T_{blk}	0.1°C
T_{in}	0.1°C
T_{orf}	0.1°C
T_{out}	0.1°C
T_{wh}	0.1°C
$T_{\text{out}} - T_{\text{in}}$	0.2°C
ΔT	0.2°C

For the data taken at a hydraulic Reynolds number of 15000 in the concave test section the following additional uncertainties applied:

Quantity (P)	Uncertainty ($\pm P$)
P_1	0.05
ΔP	0.10

The results of the uncertainty calculations at a Reynolds number of 15000 in the concave test section were:

Quantity (B)	Uncertainty ($\pm \delta B$ B)
ρ	.00445
\dot{m}	.00544
Q_{air}	.02397
\bar{h}	.02431
\overline{Nu}_{hd}	.04620
Re_{hd}	.05703

The major contribution to experimental uncertainty in both the average Nusselt number and hydraulic Reynolds number was the uncertainty in cross sectional area of the channel. The hydraulic diameter of the channel was a function of channel cross sectional area, resulting in a relatively large uncertainty in the hydraulic diameter. These two parameters accounted for approximately forty percent of the uncertainty in the average Nusselt number calculation, and about eighty percent of the uncertainty in the calculated hydraulic Reynolds number.

LIST OF REFERENCES

1. Lord Rayleigh, "On the Dynamics of Revolving Fluids," *Proceedings of the Royal Society of London, Series A*, V. 93, pp. 148-154, 1916. Reprints in *Scientific Papers*, V. 6, pp. 447-453.
2. Taylor, G.I., "Distribution of Velocity and Temperature Between Concentric Rotating Cylinders," *Proceedings of the Royal Society of London, Series A*, V. 151, pp. 494-512, 1935.
3. Schlichting, H., *Boundary Layer Theory*, Seventh Edition, pp. 529-536, McGraw-Hill, 1979.
4. Dean, W.R., "Fluid Motion in a Curved Channel," *Proceedings of the Royal Society of London, Series A*, V. 121, pp. 402-420, 1928.
5. H. Gortler, "On the Three Dimensional Instability of Laminar Boundary Layers on Concave Walls," *National Advisory Committee for Aeronautics, Technical Memorandum 1375*, 1942.
6. Yih, C.S., and Sangster, W.M., "Stability of Laminar Flow in Curved Channels," *Philosophical Magazine, Series 8*, V. 2, pp. 305-310, 1957.
7. Kelleher, M.D., Flentie, D.L. and McKee, R.J., "An Experimental Study of the Secondary Flow in a Curved Rectangular Channel," *Journal of Fluids Engineering*, V. 102, pp. 92-96, 1980.
8. Cheng, K.C. and Akiyama, M., "Laminar Forced Convection Heat Transfer in Curved Rectangular Channels," *International Journal of Heat and Mass Transfer*, V. 13, pp. 471-490, 1970.
9. Holihan, R.G., Jr., *Investigation of Heat Transfer in Straight and Curved Rectangular Ducts for Laminar and Transition Flows*, Master's Thesis, Naval Postgraduate School, Monterey, California, June 1981.
10. Shah, R.K. and London, A.L., *Laminar Flow Forced Convection in Ducts*, Supplement 1, pp. 305-312, Academic Press, 1978.
11. Brinich, P.F. and Graham, R.W., "Flow and Heat Transfer in a Curved Channel," *NASA Technical Note No. TN-D-8464*, 1977.
12. Kreith, F., "The Influence of Curvature on Heat Transfer to Incompressible Fluids," *Trans. ASME*, V. 77, pp. 1247-1256, 1955.
13. Uchida, Y. and Koizumi, H., *Forced Convective Heat Transfer in a Curved Channel with a Rectangular Cross Section*, *Trans. Japan Soc. of Mech. Engrs.*, No. 399, pp. 1708-1717, 1980.

14. Galyo, G.G., *Experimental Investigation of Turbulent Heat Transfer in Straight and Curved Rectangular Ducts*, Master's Thesis, Naval Postgraduate School, Monterey, California, December 1985.
15. The American Society of Mechanical Engineers, in Chapter 4, "Flow Measurement", of *Supplement to the ASME Power Test Codes*, 1959.
16. MINITAB, Inc., *MINITAB (computer software)*, 3081 Enterprise Dr., State College, Pennsylvania, 1985.
17. Wilson, J.L., *Experimental Investigation of Turbulent Heat Transfer in Straight and Curved Rectangular Ducts*, Master's Thesis, Naval Postgraduate School, Monterey, California, December 1984.
18. Kays, W.M. and Leung, E.Y., "Heat Transfer in Annular Passages-Hydrodynamically Developed Turbulent Flow with Arbitrarily Prescribed Heat Flux," *International Journal of Heat and Mass Transfer*, V. 6, pp. 507-537, 1963.
19. McKee, R.J., *An Experimental Study of Taylor-Gortler Vortices in a Rectangular Channel*, Eng. Thesis, Naval Postgraduate School, Monterey, California, June 1973.
20. Durao, M. do Carmo, *Investigation of Heat Transfer in Straight and Curved Rectangular Ducts Using Liquid Crystal Thermography*, Eng. Thesis, Naval Postgraduate School, Monterey, California, June 1977.
21. Ballard, J.C. III, *Investigation of Heat Transfer in Straight and Curved Rectangular Ducts*, Master's Thesis, Naval Postgraduate School, Monterey, California, September 1980.
22. Daughety, S.F., *Experimental Investigation of Turbulent Heat Transfer in Straight and Curved Rectangular Ducts*, Master's Thesis, Naval Postgraduate School, Monterey, California, September 1983.
23. Kline, S.J. and McClintock, F.A., "Describing Uncertainties in Single-Sample Experiments," *Mechanical Engineering*, V. 75, pp. 3-8, January 1953.

INITIAL DISTRIBUTION LIST

	No. Copies
1. Defense Technical Information Center Cameron Station Alexandria, Virginia 22304-6145	2
2. Library, Code 0142 Naval Postgraduate School Monterey, California 93943-5002	2
3. Department Chairman, Code 69 Department of Mechanical Engineering Naval Postgraduate School Monterey, California 93943-5000	1
4. Professor M.D. Kelleher, Code 69Kk Department of Mechanical Engineering Naval Postgraduate School Monterey, California 93943-5000	2
5. Lieutenant J.R. Hawk III 6817 W. 87th. Avenue Crown Point, Indiana 46307	2

END

7-87

DTIC